Leaf area phenology across mire types in response to meteorological variation and experimental water level manipulation

Jack Chapman

Master's Thesis

University of Helsinki

Master's Program of Forest Sciences

Forest Ecology and Management

April 2022

Abstract

Faculty: Agriculture and Forestry

Degree programme: Forestry Department

Study track: Forest Ecology and Management

Author: Jack Chapman

Title: Leaf area phenology across mire types in response to meteorological variation and experimental water level manipulation

Level: Master's Thesis

Month and year: April 2022

Number of pages: 57

Keywords: Peatland, Mire, Leaf Area Phenology, Drought, Climate Change

Supervisor or supervisors: Harri Vasander, Eeva-Stiina Tuittila, Aino Korrensalo, Egle Köster

Where deposited: Helsinki University Library

Additional information:

Abstract: Climate change is expected to cause long-term drying on northern peatlands due to increased evapotranspiration. Summer heatwaves and droughts are also predicted to increase with climate change. Vascular plant leaf area phenology on peatlands is affected by reduced water levels and interannual variation in weather. Nutrient rich mire types are more susceptible to both functional and compositional changes in response to long-term and short-term changes in water level. What remains unexplored is the potential for interactive effects between long-term drying and short-term drought events on leaf area phenology on varying mire types. This study quantifies the response of leaf area phenology to 20-year experimental water level drawdown (WLD) across three mire types of varying nutrient levels (mesotrophic fen, oligotrophic fen and ombrotrophic bog). Measurements were conducted in two contrasting growing seasons, 2017 a cool wet year and 2021 a hot dry year. WLD led to significantly earlier growth peaks across all sites. Community compositional changes in response to WLD were most significant at the more nutrient rich mire sites. At the mesotrophic site WLD resulted in significant reductions in peak leaf area (LAIMAX), which was not observed at the other sites. Across all the WLD plots the hot dry year 2021 resulted in significantly greater LAIMAX relative to the cool wet year 2017, this difference was not significant at any of the control plots. This suggests long-term drying alters the way mire phenology responds to short-term variations in weather. This has important implications for the ability of northern mires to function 'normally' under future climate conditions.

CONTENTS

1 INTRODUCTION

1.1 Background

On peatlands, anoxic conditions, resulting from a high water level, enforce slow rates of decomposition. Due to this, relatively slow photosynthetic rates are enough to maintain undrained peatlands, i.e. mires, as both sinks and significant stores of carbon (C). Global peatlands represent around 3% of the terrestrial surface area, however they are estimated to contain more than 600Gt of C, of which northern peatlands account for roughly 550GtC (Yu et al. 2010, Yu et al. 2011). Overall, northern peatlands also remain a persistent sink of C and have a net negative effect on radiative forcing of climate change despite methane emissions (Frolking et al. 2006). However, the balance between C accumulation and release is delicate, and in many instances environmental change may tip mires into net C emitters (Silvola et al. 1996, Dorrepaal et al. 2009, Couwenberg et al. 2011). Increased temperatures, increased litterfall and lower water tables may lead to accelerated rates of mineralisation of previously stable C pools (Dorrepaal et al. 2009). Though, in some instances the same changes may result in increases in photosynthetic productivity that balances these effects (Lohila et al. 2011, Munir et al. 2014). Understanding the response of mires to environmental change is key to maintaining them as C stores and sinks and in building accurate climate models that consider potential feedback mechanisms.

The impacts of climate change are predicted to be particularly profound at high latitudes, where northern mires are found. Boreal ecosystems will see increased temperatures, though the impacts on precipitation are more variable and uncertain (Monier et al. 2013). Regardless, higher temperatures will lead to increased evapotranspiration within mires and in surrounding upland catchments. In many mire systems this will result in reduced water balances (Helbig et al. 2020). Mire ecosystems are primarily defined by hydrological regimes and as such changes to hydrology can result in drastic changes to ecosystem structure and functionality (Tahvanainen 2011). Additionally, surface height above water is a key driver of microvariation in plant distribution on mires (Tuittila et al. 2007). Mire water tables affect plant distribution through nutrient availability due to variation in mineralisation rates or presence of nutrients in groundwater and through the presence of structural adaptations like aerenchyma, as a response to anoxic conditions.

Due to the key role of high water tables in peatland systems, if lower water tables and aerobic soil conditions result in increased nutrient availability, peatland communities may shift towards more forest associated species and increased tree growth at the expense of specialised mire vegetation. Greater tree growth will also increase shading and may have the effect of further lowering the water table through accelerated transpiration rates (Kokkonen et al. 2019). Alternatively, water level drawdown (WLD) may disconnect vegetation on fens from lateral flow of minerogenic water. Nutrient availability may decline and without a steady source of cations to buffer organic acids, pH will decrease (Laine et al. 2004). This process of ombrotrophication may see sedge-dominated fen vegetation replaced by bog *Sphagnum* species within decadal timescales (Tahvanainen 2011, Wu and Roulet 2014).

Major successional shifts of mire communities like forest-encroachment or ombrotrophication represent substantial changes in the relative dominance of plant functional types (PFTs) that also suggest long-term shifts in the functioning of mires. Crucially, differences in characteristics and growth strategies between PFTs may affect C cycling (Rupp et al. 2019). For example, sedges may play a disproportionate role in C sequestration due to their production of root litter (Laiho et al. 2003). Conversely, plants adapted to anoxic conditions, like sedges, have aerenchyma which are believed to be one of the primary means of methane transport to the atmosphere (Green and Baird 2012). Additionally, it is still not well understood, how large a role plant diversity on mires plays in maintaining C sequestration (Korrensalo et al. 2017). Different functional groups have varying photosynthetic strategies in response to seasonality and environmental conditions and furthermore, the quality of plant litter is also a major control on decomposition rates (Straková et al. 2012, Wang et al. 2021). Therefore, more diverse functional assemblages may provide greater consistency in C sequestration, despite yearly environmental variation.

Resilience in C sequestration as an ecosystem trait may reflect variation in phenological strategy between species (Korrensalo et al. 2017). Phenology is now recognised as a key regulator of C cycling in peatlands, additionally acting as intermediary for abiotic factors (Wilson et al. 2006, Koebsch et al. 2019). Consequently, phenological measures also function as effective predictors of C fluxes on mires (Kross et al. 2014, Peichl et al. 2015). In this regard leaf area index (LAI) development is the aspect of phenology that receives most research focus. LAI is relatively easy to measure and the amount of photosynthetic area functions as a baseline limiting ecosystem production and is also likely an important determinant of autotrophic

respiration and even heterotrophic respiration through litter inputs (Wilson et al. 2006, Peichl et al. 2015, Koebsch et al. 2019).

1.2 Synthesis of previous research

Previous research (Mäkiranta et al. 2018) has found clear evidence that leaf area phenology is susceptible to change in response to moderate WLD (3 – 7 cm), but the response is different between PFTs. On the studied fen sites WLD drawdown led to increased seasonal maximum leaf areas (LAIMAX) for shrubs and decreased LAIMAX for forbs and sedges. The WLD treatment also led to a longer growing season, due to both the shift towards shrubs and a lengthened growing season for sedges. Since the dominance of PFTs varies between mire ecosystem types it is reasonable to assume that the impacts of WLD on phenology may similarly vary. Research already suggests that resilience to climate driven environmental change varies between mire community types, with richer and wetter sites most vulnerable to changes in species composition (Weltzin et al. 2003, Kokkonen et al. 2019). Over a 5-year timescale mesocosm study, Weltzin et al. (2003) found that WLD led to increases in shrubs and decreases in graminoids at both bogs and fens but the changes were more pronounced at fens. Similar results have also been observed from ecosystem manipulation studies; Kokkonen et al. (2019) established that experimental WLD leads to more dramatic changes within the fen communities than at the bog over the first 15 years. While only slight changes in the hollow communities were detected at the ombrotrophic site, microtopography of the mesotrophic fen site became homogenised and the community shifted towards forest associated species (Kokkonen et al. 2019).

Outside of climate driven successional changes on mires, interannual meteorological variation is also known to have contrasting effects on the functioning of different mire types. Summer drought periods and heatwaves will occur with increasing frequency in response to climate change across Europe (Füssel et al. 2017). Richer mire types appear to be more sensitive to temperature increases, since bogs are likely to have negative feedback mechanisms reducing the temperature through increased evapotranspiration regardless of water level, although these results come from a single mesocosm experiment (Bridgham et al. 1999). This complements what is known about how interannual meteorological variation has differential impacts on C cycling between mire types. Yearly gross primary production (GPP) rates are more variable in response to weather at richer mire sites, dominated by sedges, compared with poorer sites, dominated by *Sphagnum* or ericaceous shrubs (Bubier et al. 2003, Adkinson et al. 2011,

Leppälä et al. 2011). Water table and temperature appear to be the key drivers of this variation Adkinson et al. 2011). Warm dry growing seasons reduce C uptake on all mire types due to elevated ecosystem respiration rates, however only the sedge fens seem to show significant decreases in photosynthesis rates during dry periods, connected with earlier senescence of the sedges (Bubier et al. 2003). However, GPP can increase on fens in response to moderately drier conditions and early senescence in sedges only occurs during pronounced drought (Sulman et al. 2010). This suggests plant growth on fens may benefit from increased temperatures and mineralisation in drier conditions but there is a hard threshold for water tables below which growth is negatively affected. Although, it is notable that Macrae et al. (2013) found no clear changes in mineralisation rates in response to WLD on either a poor fen or bog, suggesting other drivers may be more important. Indeed, recent research has suggested that nutrient poor mires may maintain slow decomposition rates regardless of lowered water levels through the interaction between the plant litter quality and soil biota (Wang et al. 2021).

While it is well established that richer mire types are both more vulnerable to successional shifts in response to long term climate driven drying and to changes in functionality in response to interannual meteorological variation, the potential interaction between the two (drying induced successional change and interannual meteorological variation) on different mire types has not been explored previously. Further, the effect of these drivers on leaf area phenology has not been established. Leaf area phenology is only one aspect of mire functionality; however, it is recognised as a key predictor of C fluxes on peatlands (Wilson et al. 2006, Kross et al. 2014, Peichl et al. 2015, Koebsch et al. 2019). The relative resilience and potential successional changes on different mire types in response to environmental stresses are important to understand in light of potential feedbacks to the climate and threats to peatland biodiversity.

1.3 Objectives and Hypotheses

The object of this study is to understand how climate change stresses are likely to impact the leaf area phenology of boreal peatlands. I aim to quantify the response of leaf area phenology of vascular plants to long term WLD across three mire types with varying nutrient levels, over two growing seasons with contrasting meteorological conditions. Additionally, I will look for differences in the community structure between control sites and sites that have experienced two decades of experimental WLD.

I will apply experimental long term WLD as a proxy for changing mire water tables and successional changes resulting from baseline climate shifts. Measurements across two contrasting growing seasons, one cooler summer with consistent precipitation and one hotter summer with a pronounced drought period, are included to address the impacts on phenology of potential increased interannual variation within the future climate. The study is conducted across a range of mire types defined by nutrient status, with the purpose of better understanding variation in vulnerability within boreal mires.

Understanding the underlying species changes serves to assist in explaining observations in leaf area phenology, explicitly connecting study of ecosystem functioning to community composition, which has been identified as an area in need of development (Loreau 2010). It also serves as an update on the successional dynamics described in Kokkonen et al. (2019), that explored the community changes at the same study site up until 2016.

Based on earlier findings (Mäkiranta et al. 2018), I hypothesised that WLD will increase the length of growing seasons across the study sites, due to both an increased presence of shrubs, which have longer growing seasons relative to forbs, and extended growing seasons for sedges. Similarly, to Mäkiranta et al. (2018), I also expected to find decreased LAIMAX in response to WLD related to a larger decrease in forbs and sedges than increase in shrubs. I expected this effect to be more pronounced since the timeframe of WLD in this study is longer than in Mäkiranta et al. (2018).

Overall, I expected that the leaf area phenology of the richer mire types would be more responsive to WLD but that the nature of long-term community compositional changes on WLD plots would result in them being less responsive to interannual meteorological variation relative to control plots. This last prediction reflects the relative shifts in PFT dominance observed in response to drying on mires and the phenology of those PFTs in response to meteorological variation (Bubier et al. 2003, Kokkonen et al. 2019).

2 METHODS

2.1 Study sites and plot design

To study the impact of long-term water level drawdown (WLD) I applied experimental drainage at Lakkasuo, a peatland located near Orivesi, Finland (61°47′N, 24°18′E). The

average annual temperature is 3.5°C and annual precipitation is 711mm (ICOS 2018). This is a raised eccentric bog complex, on the border of the Southern and Middle boreal climatic zones in Finland (Ahti et al. 1968). Characteristic to raised eccentric bogs, it has an ombrotrophic centre, located in the southern end of the peatland. The complex also includes substantial areas of fen fed by groundwater from an adjoining esker, in the northern half of the mire (Laine et al. 2004). The hydrology of the site has remained natural compared with most mire complexes in Southern Finland, although it is not entirely unaffected by human activity (Laine et al 2004). Due to its wide range or mire site types and natural condition, Lakkasuo has been used for teaching purposes and research into mire ecology since the 1960s. As such, the characteristics of the site are already well documented.

The eastern part of the mire was drained for forestry purposes in 1961. The nutrient gradient of the mire broadly runs South-North, the area of drainage ditches runs parallel to this, cutting across the wide gamut of mire types present at the site (Laine et al. 2004) (Figure 1). The WLD experimental design was established adjacent to this since it allows comparison with the forestry drainage areas and easy drainage into the existing ditch network. For the WLD treatment, shallow ditches were constructed at three sites each representing different mire nutrient statuses characteristic to northern peatlands: rich fen (mesotrophic) (Figures 2 and 3), poor fen (oligotrophic) (Figures 4 and 5), and bog (ombrotrophic) (Figure 6). The ditching was carried out in spring 2001 for the mesotrophic and ombrotrophic sites and spring 2002 for the oligotrophic site. Prior to the ditching the mesotrophic and oligotrophic WLD treatment plots were not significantly different from their respective control plots, though the ombrotrophic treatment plots differed slightly (Kokkonen et al. 2019).

The ditching was achieved by encircling a 25 x 15 m rectangle in 30 cm deep ditches and then linking this area to the nearby deeper forestry drainage. The ditching has successfully resulted in an 8 - 14 cm reduction in water tables relative to the controls for all mire types since the start of the experiment (Kokkonen et al. 2019). Ditches have been cleaned periodically. There is only one WLD treatment plot for each mire type, due to resource limitations and difficulty in finding sites with the same nutrient status and vegetation characteristics. As such, sample plots within each treatment plot are pseudo-replicates. Within each of the 6 treatment plots, 8-10 permanent pseudo-replicated square sample plots were established, measuring 56 x 56 cm. The sample plots are surrounded by wooden walkways to prevent footfall damage to vegetation and peat. In the case of the mesotrophic drained site, sample plots were 30 cm diameter circles.

This was due to the difficulty in establishing the larger collars permanently where the trees had grown more rapidly and densely.

Figure 1. Aerial view of Lakkasuo mire complex, showing the locations of the studied mire types. WLD ditched areas are directly adjacent to control sites. The forestry drainage is visible in the wooded areas directly to the East of the open mire areas. Mes = mesotrophic fen; Oli = oligotrophic fen; Omb = ombrotrophic bog.

All the study sites started as open peatlands containing only stunted trees. Since the drainage experiment tree cover has increased at the mesotrophic drained treatment plot (Figure 2) and to a lesser degree at the oligotrophic drained treatment plot (Figure 4). Consequently, these treatment plots experience additional shading compared with the respective control treatment plots. Prior to the drainage experiment the ombrotrophic site contained substantial microtopography, including hummocks, lawns, and hollows, with corresponding variation in the vegetation community (Figure 6). The vegetation was comprised of mostly *Sphagnum*,

Eriophorum vaginatum and several dwarf shrub species (Laine et al. 2004, Kokkonen et al. 2019). The oligotrophic site contained mostly lawn-level vegetation, composed of a ground cover of *Sphagnum*, particularly *Sphagnum papillosum*, and a field layer of sedges with some forbs and dwarf shrubs (Laine et al. 2004, Kokkonen et al. 2019) (Figure 5). The mesotrophic site exhibited some topography with a mix of hollow and lawn level plant communities (Figure 3). The field layer was also dominated by sedges, particularly *Carex lasiocarpa*. There was less *Sphagnum* ground cover relative to the oligotrophic site, but many more herbaceous plants present (Laine et al. 2004, Kokkonen et al. 2019).

Figure 2. Mesotrophic WLD site. ©Noora Dahlman

Figure 3. Mesotrophic control site. ©Noora Dahlman

Figure 4. Oligotrophic drained site. ©Laura Koivu

Figure 5. Oligotrophic control site. ©Laura Koivu

Figure 6. Ombrotrophic control site. ©Laura Koivu

2.2 Meteorological data

Meteorological data was obtained from the weather station at Hyytiälä (61°47′N, 24°18′E), which is situated 6km to the north of the site. Used data included: temperature, precipitation, photosynthetically active radiation levels (PAR) and snow cover. All measurements were automatic recordings every minute over the course of the season. Temperature measurements were taken from a height of 4.2m using Pt100 inside a ventilated shield. Precipitation was recorded as accumulated precipitation over the previous minute using a Vaisala FD12P sensor at 18m height. PAR measurements were recorded from a 35m tower using a Li-Cor Li-190SZ quantum sensor. Snow depth data comes from a nearby open field site and was recorded using a laser snow depth sensor (Jenoptik SHM30).

2.3 Sample plot characterisation

The water table depth in relation to moss surface was monitored at the same time as leaf area measurements from permanent perforated PVC tubes installed into the peat next to each sample plot. Marked plastic tubing was inserted inside and blown down to determine the level of the water.

Percentage cover measurements were taken during the growing season in 2021 to characterise the species composition of each sample plot. Estimates were made using a grid overlay and represent a consensus judgement between researchers. Percentage cover of vascular plants was measured close to the peak of the growing season 6th – 13th July. However, bryophytes were measured later in the season since they were too dry to readily identify in July 2021, instead bryophyte cover estimates are from 23rd – 29th September 2021.

2.4 Leaf area measurements

Data for leaf area index (LAI) was collected during the growing seasons of both 2017 and 2021. Measurements started near the onset of the growing season, in early May and concluded during the senescent period, in late August or September. In 2017 six measurements taken, in 2021 five measurements were taken. Measurements were spaced throughout the growing season.

The LAI (m^2 m^{-2}) for individual vascular plant species was estimated using a method previously developed by Wilson et al. (2006). This involved counting leaves in study plots at intervals throughout the active season and using species and time specific average leaf area. Average leaf area for species was determined at the time of each leaf count by harvesting plants from outside the study plots, but within the study site. These samples were then measured in the lab using an electronic area meter. With some species, conversion formulas were applied to correct for spherical or hemi-spherical forms. Both Wilson at al. (2006) and Mäkiranta et al. (2018) found no difference between this method and manual leaf area measurements.

Within each sample plot the leaf counts were taken from five sub-plots of 8 x 8 cm, situated in the corners and centre of the plot. The positioning of the sample plots remained fixed between 2017 and 2021. Sub-plots were positioned to be representative of the vegetation present in the plot. Infrequent, unevenly distributed, and larger species were instead counted over the entire plot. At the mesotrophic drained treatment plot, where the sample plot sizes were different, no sub-plots were used, and all species were counted over the entire circular sample plot. For certain species it was more appropriate to measure by length than to count leaves, e.g., *Vaccinium oxycoccos* and *Betula nana*. In these cases, protocols were established for each individual species to ensure length measurements were consistent. Consequently, the corresponding average leaf area measurements also used length rather than leaf count.

Re-assignation of species identification was necessary on a few occasions, particularly where early season growth of Poales species were difficult to identify. By using later season measurements, when distinguishing features became more visible, it was possible to correct species identification with a high degree of certainty.

Species leaf counts per plot were multiplied by average leaf area to generate a single leaf area per area measure (m^2 m^{-2}) for each species on each plot for each measurement day. Values for species were then combined to form LAI for vascular plants at each plot.

2.5 Data processing

Growing degree days (GDD) were calculated from average daily temperatures. A base of 5°C was used based on Rana and Tolvanen (2021). Average temperatures were also capped at 30°C on the assumption that temperature is unlikely to limit photosynthesis after this point, however

at no point did mean temperatures exceed this threshold. The thermal growing season was assumed to start from the first period when temperatures were above 5°C for five consecutive days and snow cover had melted from open areas. This was 2nd May in 2017 and 17th April in 2021.

A simple monthly water balance model was constructed to show purely inputs and outputs to and from the atmosphere, the difference between total precipitation and potential evapotranspiration (PET). Monthly PET was calculated in a simplified formula from Skov and Svenning (2004)

$$PET = 58.93 \times monthly\ average\ temperature/12 \quad (1)$$

Water table data was linearly interpolated to fill in the gaps in measurements conducted intermittently. Original measurements were used to test for the effect of WLD on peatland water levels, with repeated measurements and sample plots controlled for as random factors.

Species percentage cover data was used to calculate functional group percentage cover and species richness. Whittaker's beta diversity (β_w) was used to compare species turnover between control and WLD sites:

$$\beta_w = \frac{S}{\alpha} - 1 \quad (2)$$

where S is total species pool and α is average site species richness.

Detrended correspondence analysis (DCA) on the percentage cover data was conducted in R using the vegan package. Natural log values were used and data was further transformed to equalise differences between species and search intensity using the decostand function. Rare species were downweighted.

2.5 Modelling leaf area phenology

From the field measurements the overall seasonal development of the LAI was modelled using a log normal function. Wilson et al. (2006) found that at Lakkasuo, and likely also across all

boreal peatlands, plant growth accelerates rapidly to a peak and then declines more slowly in the autumn. This is due to the short and intense nature of summers at high latitudes. Therefore, a log normal function is more appropriate for describing leaf area phenology than a simple normal function. Wilson et al. (2007) developed an equation that uses, as parameters, the LAI season maximum (LAIMAX), the Julian day that LAIMAX occurs (DMAX) and a unitless value representing the 'broadness' of the green season (Shape), to describe the annual development of LAI (Figure 7). Using this function, a non-linear mixed effects model was constructed to determine the linear dependence of the parameter values of the factors: year, site and water level drawdown treatment (wld), and their interactions.

$$LAI_{pm} = C + LAIMAX_p \times \exp\left(-0.5\left(\frac{\ln\left(\frac{D_{pm}-S}{DMAX_p}\right)}{Shape_p}\right)^2\right) + e_{pm};\ LAIMAX_p, DMAX_p, Shape_p > 0 \quad (3)$$

where LAI_{pm} is the observed total leaf area index and D_{pm} represents the number of days since the start of the spring growing season for measurement m at measurement plot p. C is a constant representing evergreen leaf area that exists prior to the onset of the growing season. This was fixed at 0.08 $m^2\ m^{-2}$, which was determined to be realistic in Mäkiranta et al. (2018). S is the Julian date set as the start of the growing season, fixed at day 110 (19th April) based on field observations. The residuals (e_{pm}) were found to be evenly spread around the mean of zero and are normally distributed with a constant variance. The parameters to be estimated were $LAIMAX_p$, $DMAX_p$ and $Shape_p$ and were further written as linear combinations of fixed predictors. Fixed predictors and their interactions were sequentially introduced to each parameter submodel and marginal ANOVA was used to assess whether the added predictor improved the model in comparison to the simpler model ($p<0.05$). Those variables that did not have significant predictive capacity were excluded from the final model. Where interactions between variables had a significant predictive effect, they have been retained even if the effect of the variable itself was not significant.

The final submodels included the following fixed predictors for each parameter:

$$\boldsymbol{LAIMAX_p}: year_p + wld_p + site_p + year_p * wld_p + wld_p * site_p + b_p$$

$$\boldsymbol{DMAX_p}: year_p + wld_p + site_p + year_p * site_p$$

$$\boldsymbol{Shape_p}: year_p + wld_p + site_p + year_p * wld_p + year_p * site_p + wld_p * site_p + year_p * wld_p * site_p$$

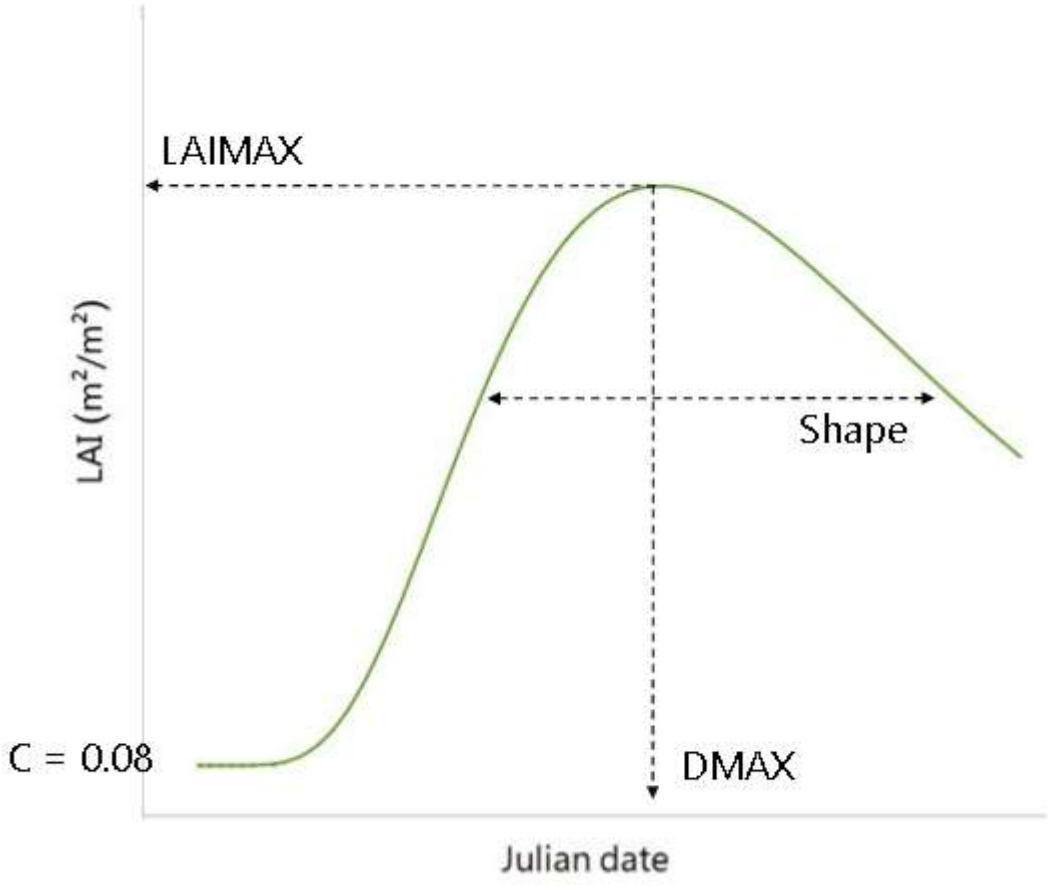

Figure 7. Example of leaf area phenology using the log normal function described above. LAIMAX is the LAI seasonal maximum. DMAX is the Julian day on which LAIMAX occurs. Shape is a unitless value representing the 'broadness' of the green season, a larger Shape value indicates a longer green season.

Random effect of permanent sample plot (b_p) was included only for LAIMAX due to convergence problems with more complex random effects structure. The model used natural logged parameter values to remove the possibility of generating negative figures for LAI.

The model was constructed in R using the nlme package.

Model pairwise comparisons of parameter means were obtained using the emmeans package (Appendix 1). The confidence intervals for non-significant effects excluded from the final model are reported in Appendix 2 from a separate model including all the variables and interaction levels.

3 RESULTS

3.1 Climatological results

The growing season in 2021 was substantially warmer than 2017 (Figure 8). Temperatures were consistently higher across from early April until mid-September, with the exception of a small temperature spike in early August of 2017. The differences in late June and early July were most pronounced. Daily maximums in 2021 peaked at 34°C on 22nd June compared with a daily maximum of only 28°C in 2017. In total, 2017 only had 2 days with daily maximums over 25°C, in contrast 2021 had 42. The difference is also evident in the growing degree days (GDD), 2021 accumulated 1444 GDD by 30th September compared to 1018 GDD in 2017, 30% less (Figure 9).

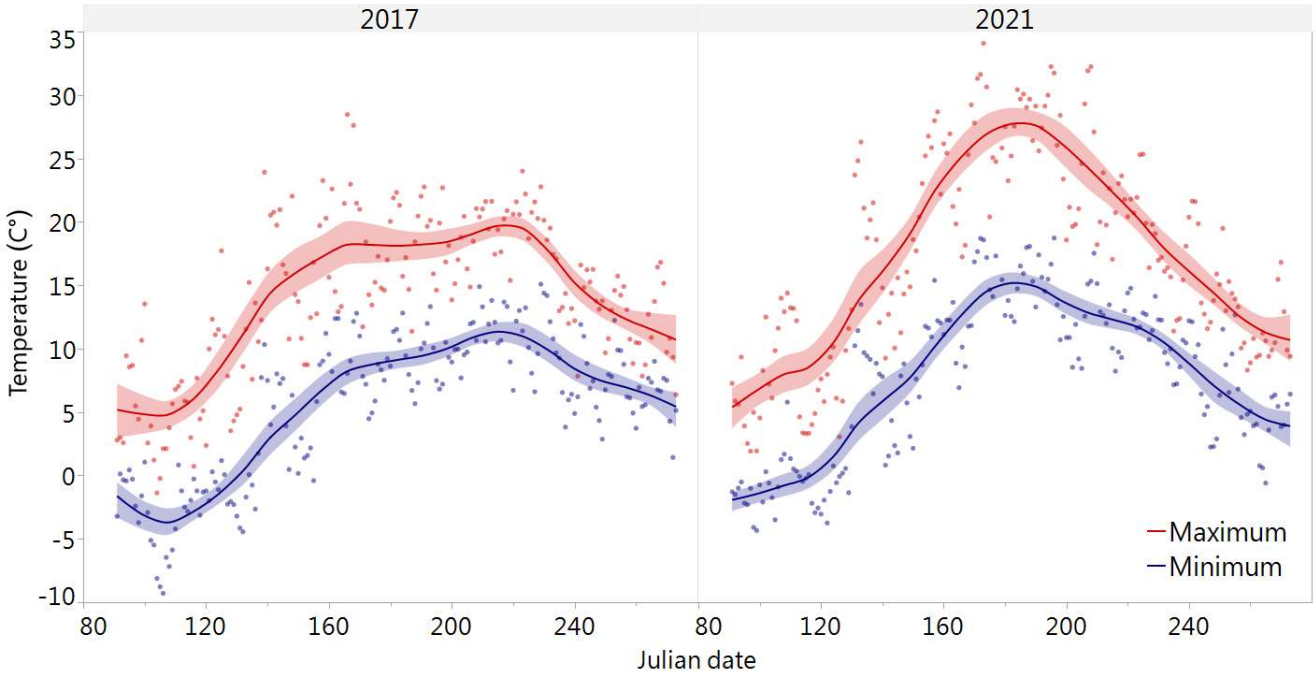

Figure 8. Daily minimum and maximum temperatures between Julian dates 91 and 273 (April-September) in 2017 and 2021. A smoothing splice has been fitted (λ = 0.05) and the shaded area

represents confidence of fit. Julian dates: 91 = 1st April; 121 = 1st May; 152 = 1st June; 182 = 1st July; 213 = 1st August; 244 = 1st September.

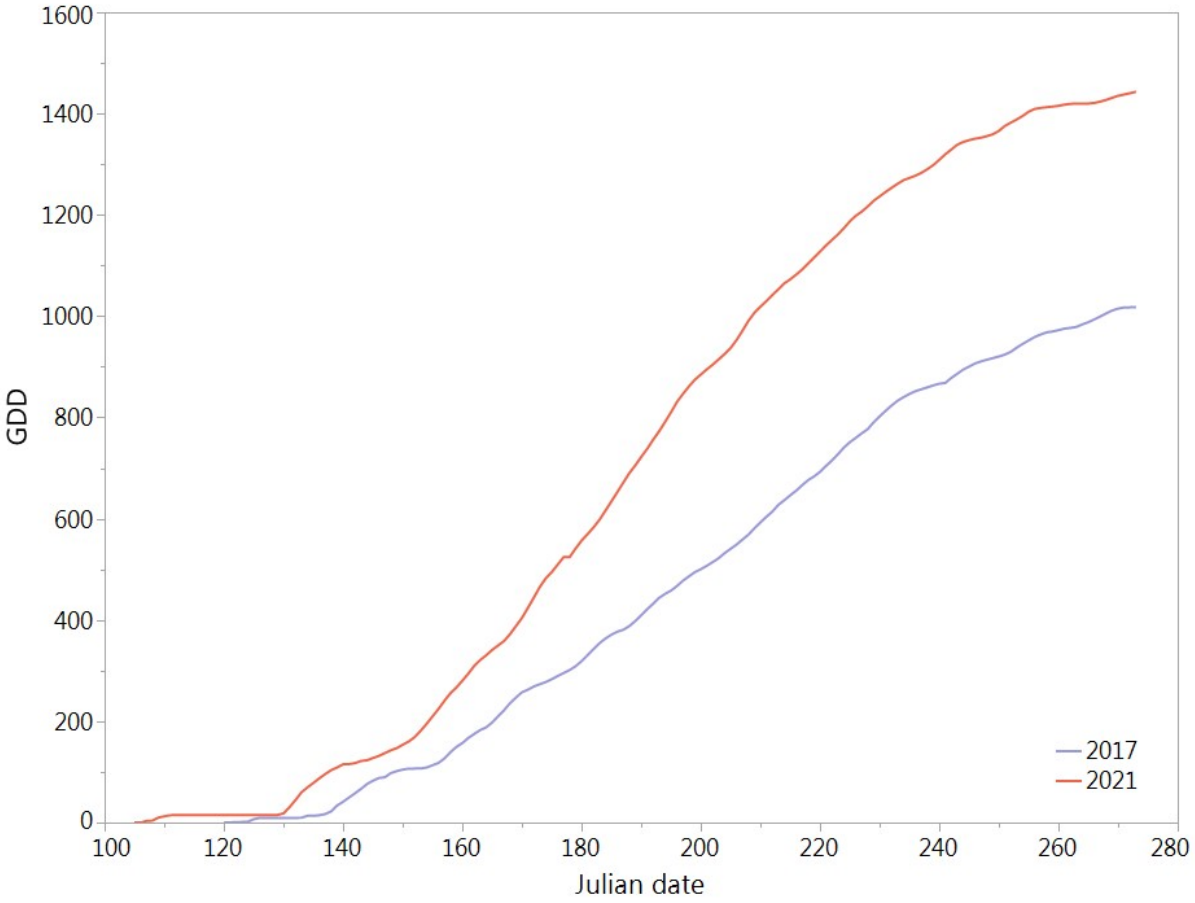

Figure 9. The accumulation of GDD from the start of the thermal growing season until Julian date 273 (30th September). The thermal growing season started on Julian date 122 (2nd May) in 2017 and Julian date 107 (17th April) in 2021. Julian dates: 91 = 1st April; 121 = 1st May; 152 = 1st June; 182 = 1st July; 213 = 1st August; 244 = 1st September.

Total precipitation from April to September was approximately the same between the two years, 475mm and 486mm respectively. However, the distribution across the growing season differed (Figure 10). In 2017, May was notably dry, and the other months showed consistent rainfall. In 2021, August was the wettest month and in midsummer there was a dry period, coinciding with the period of greatest evapotranspirative demand. This dry period was also evident in the monthly water balances where in both June and July 2021 PET exceeded precipitation (Figure 11). In 2017, the water balance was only negative in May.

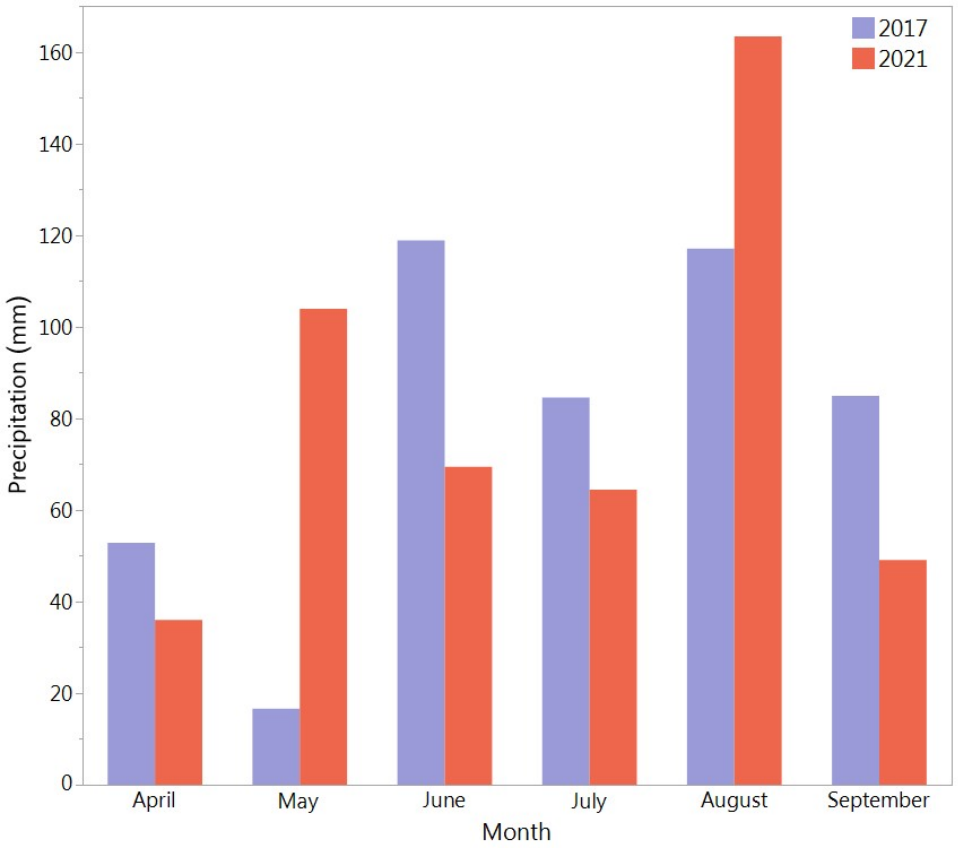

Figure 10. Total monthly precipitation April-September in 2017 and 2021.

Figure 11. Total monthly water balance based on precipitation minus potential evapotranspiration (PET).

The recorded water tables of the mire sites show an effect from the WLD ditching (Figure 12). At the oligotrophic site, WLD resulted in a -9.2 cm average reduction relative to the control site over both the years (p<0.0001). Water tables at WLD plots were also lower than control plots at the ombrotrophic (-6.4 cm, p=0.0855) and mesotrophic sites (-6.5 cm, p=0.0598), though these differences were not significant to p<0.05. There was a larger difference in water table between the mesotrophic control and WLD plots in 2021 (-7.1 cm, p= 0.0414), compared with 2017 (-5.4 cm, p= 0.1260). The was no significant difference in water level between WLD and control plots at the ombrotrophic site during either year. Across all the sites, the effect of WLD seems to be most pronounced during drying periods, when change in water levels appears to be dampened at control plots (Figure 12). The difference between control and WLD plots was significantly more pronounced across all sites in 2021 than 2017 (p= 0.0488). The drought period on the mires during June and July 2021 is evident at all of the sites, which is the clearest difference between the two years (Figure 12). Overall, the variations in water table regime between the sites are equivocal. The ombrotrophic site appears to be the wettest overall, which may be a factor in explaining why WLD had the least effect there, though differences were non-significant.

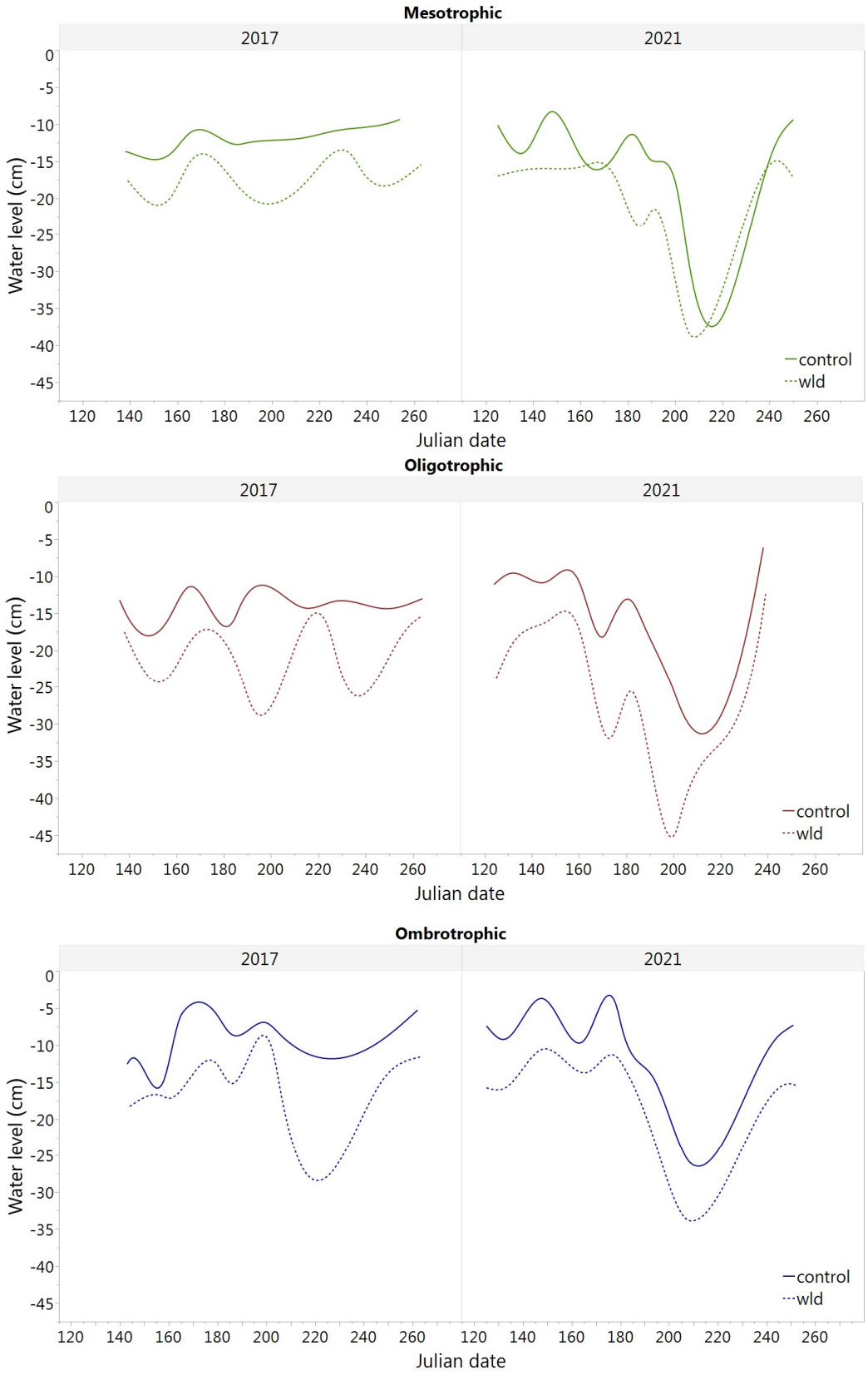

Figure 12. Water table depths below surface level across the growing season in 2017 and 2021. Start and end points of the data vary with the dates of measurement. Data has been interpolated between measurements using natural spline interpolation. The average effect of WLD was: -6.5 cm (p=0.0598) at the mesotrophic site; -9.2 cm (p<0.0001) at the oligotrophic site and -6.4 cm (p=0.0855) at the ombrotrophic site. Julian dates: 91 = 1st April; 121 = 1st May; 152 = 1st June; 182 = 1st July; 213 = 1st August; 244 = 1st September.

Daily average rates of photosynthetically active radiation (PAR) were higher during May in 2017 and higher in June and July in 2021 (Figure 13). The difference was greatest in July when 2017 monthly average was 75% of that in 2021. Total cumulative PAR across the growing season was higher in 2021, the value for 2017 was 85% of the 2021 total (Figure 14).

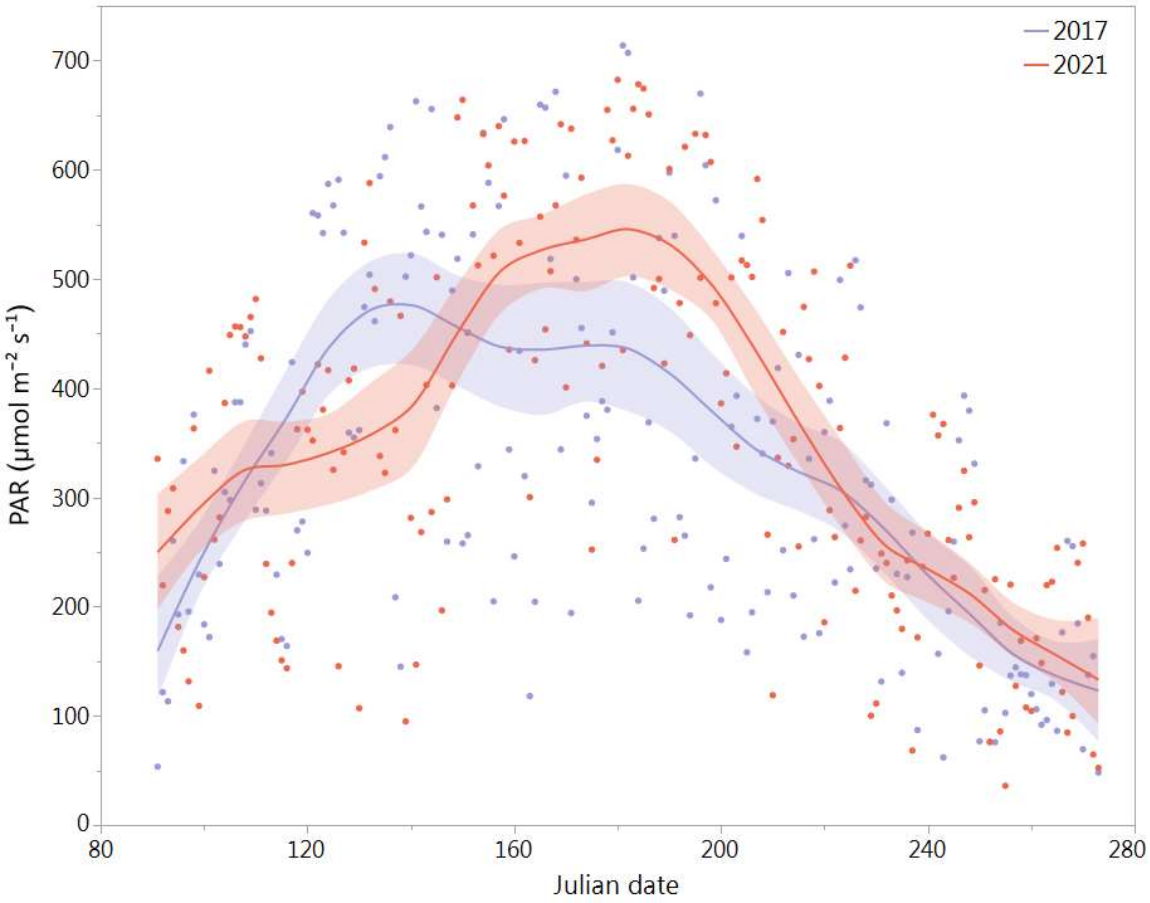

Figure 13. Daily average PAR values between Julian dates 91 and 273 (April-September) in 2017 and 2021. Days with partial data missing were excluded. Julian dates: 91 = 1st April; 121 = 1st May; 152 = 1st June; 182 = 1st July; 213 = 1st August; 244 = 1st September.

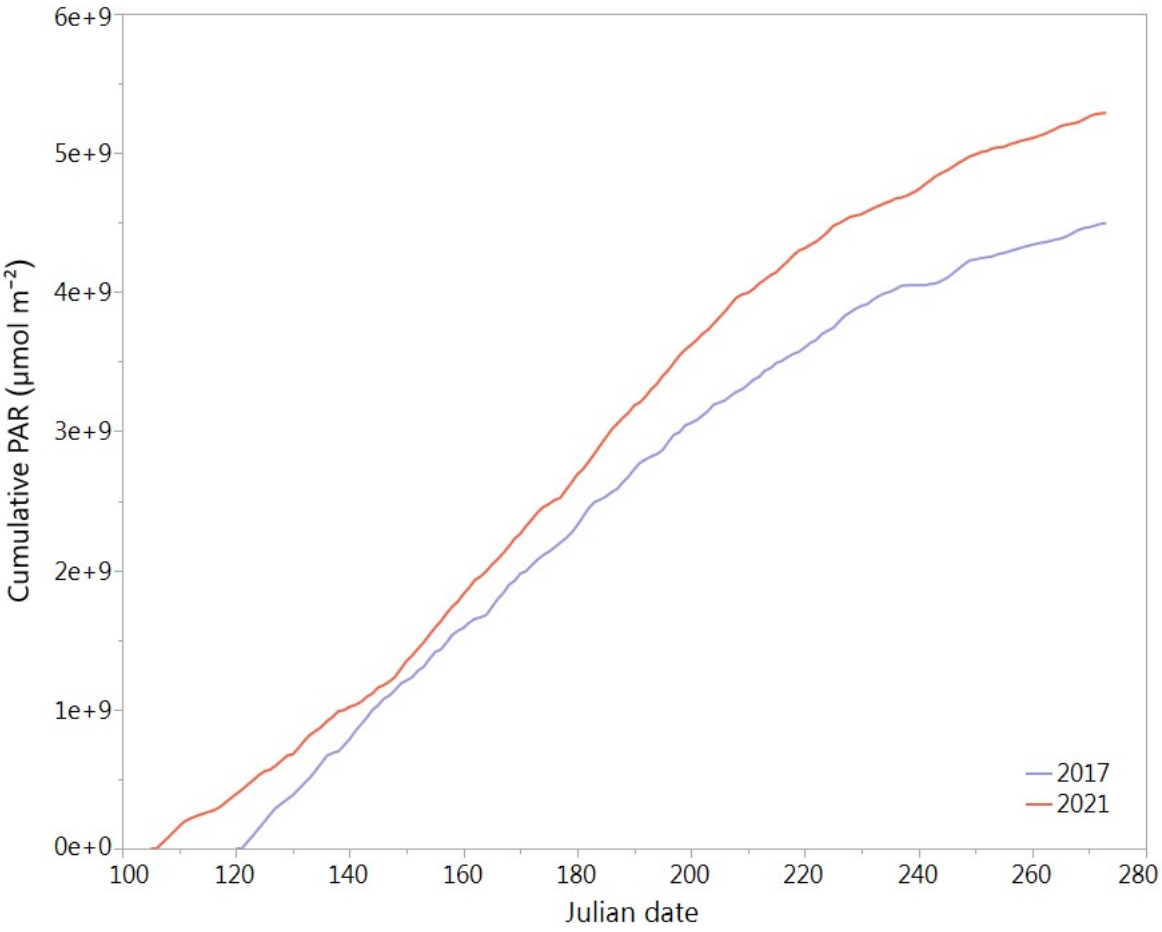

Figure 14. Total cumulative PAR from the start of the thermal growing season until Julian date 273 (30th September). The thermal growing season started on Julian date 122 (2nd May) in 2017 and Julian date 107 (17th April) in 2021. Julian dates: 91 = 1st April; 121 = 1st May; 152 = 1st June; 182 = 1st July; 213 = 1st August; 244 = 1st September.

3.2 Impact of WLD on species composition

The three sites and their treatment plots differed in the abundance of different functional groups (Table 1). The ombrotrophic and oligotrophic sites had higher levels of bryophyte cover than the mesotrophic site (Table 1). The ombrotrophic WLD plot had the highest bryophyte cover, although not significantly higher than the control plot. At the mesotrophic and oligotrophic sites there was also no difference in bryophyte cover between the WLD and control plots. However, a greater proportion of the bryophytes were *Sphagnum* species at the control plots. For the ombrotrophic sites almost all bryophyte cover was *Sphagnum*, regardless of the drainage status.

Table 1. Average percentage cover of plant functional groups in understory vegetation across the three sites and their control and WLD treatment plots. *P* values are from Welch's t-test conducted on natural log values. Bryophytes were measured 23rd-29th September 2021 and vascular plants were measured 6th-13th July 2021.

Treatment plot	Bryophytes				Vascular plants												Total plants	
	Sphagnum		**Total**		Sedges		Grasses		Evergreen shrubs		Deciduous shrubs		Forbs		**Total**			
	%	*p*	%	*p*	%	*p*	%	*p*	%	*p*	%	*p*	%	*p*	%	*p*	%	*p*
Meso control	60.0	*0.67*	62.1	*0.77*	12.3	*0.01*	-	*0.3*	19.5	*0.03*	6.0	*0.04*	4.6	*0.93*	42.4	*<0.01*	104.5	*0.13*
Meso WLD	53.1		63.3		4.5		2.1		1.1		0.6		4.3		12.7		76.0	
Oligo control	72.8	*0.24*	78.4	*0.75*	11.3	*0.05*	-		9.6	*<0.01*	8.1	*<0.01*	1.2	*0.17*	30.2	*<0.01*	108.6	*0.01*
Oligo WLD	61.5		77.0		4.0		-		31.1		20.0		0.1		55.1		132.1	
Ombro control	75.6	*0.26*	75.6	*0.26*	2.2	*<0.01*	-		3.1	*0.02*	0.4	*0.89*	2.5	*0.75*	8.2	*0.02*	83.7	*0.18*
Ombro WLD	86.3		86.4		6.4		-		9.7		0.3		2.1		18.6		105.0	

Both mesotrophic and oligotrophic WLD plots had substantially reduced cover of sedge species in comparison with the controls (Table 2 and 3). At the ombrotrophic site there were no true sedge species (*Carex*), but the pattern was reversed for Cyperaceae overall, with increased presence of *Eriophorum vaginatum* at the WLD site and a large clump of *Trichophorum cespitosum* growing in one sample plot (Table 4). The mesotrophic WLD plot was the only location where Poaceae species were present (Table 2). The oligotrophic WLD had the highest cover of both evergreen and deciduous shrubs (Table 3). In contrast, in the mesotrophic site, the control plot had greater shrub cover. However, it is worth stressing that only the ground level vegetation was surveyed and at the mesotrophic WLD plot, rather than declining, many of the shrubs have become trees since the onset of the drainage experiment. At the ombrotrophic site the WLD plot had a greater cover of evergreen shrubs relative to the control plot. The cover of deciduous shrubs was uniformly low across the ombrotrophic site and only *Vaccinium uliginosum* was present (Table 4). Forbs were most prevalent at the mesotrophic site, followed by the ombrotrophic site. The oligotrophic control plot had low forb cover, but still substantially higher than the WLD, where only scattered *Drosera rotundifoli*a were present (Table 3).

Sphagnum angustifolium and *Sphagnum fallax* dominated the bryophyte community at the mesotrophic control plot, though neither are present in all sample plots (Table 2). At the WLD

plot the bryophyte community was more evenly spread and no species was dominant across more than two sample plots. Several woodland associated bryophyte species were only present at the WLD plot, notably *Dicranum polysetum*, *Rhytidiadelphus subpinnatus* and *Sphagnum russowii*. Overall, the vascular plant community at the mesotrophic site was the most diverse of any site and no species dominated the community. *Betula nana*, *Carex lasiocarpa* and *Vaccinium oxycoccos* were the only species present in all control sample plots. Vascular plant coverage at the WLD plot was sparser, and no species occurred in all sample plots. *Carex echinata* was the most consistently present while *Agrostis spp.* and *Trientalis europaea* had high cover in some sample plots. Many of the species prevalent in the control plot were absent or almost absent at the WLD plot, notably *Andromeda polifolia*, *B. nana*, *C. lasiocarpa* and *Carex rostrata*.

Table 2. Percentage cover of bryophytes (measured 23rd-29th September 2021) and vascular plants (measured 6th-13th July 2021) at the **mesotrophic** site. The two most abundant bryophytes and vascular plants are highlighted in bold.

Species	Control plot								WLD plot							
	1	2	3	4	5	6	7	8	1	2	3	4	5	6	7	8
Aulacomium palustre	1	6	1	-	0.1	-	-	0.1	**15**	12	-	-	-	0.1	-	1
Dicranum polysetum	-	-	-	-	-	-	-	-	0.1	0.2	-	**12**	**29**	-	-	-
Marchantiophyta spp.	-	-	-	-	-	-	-	-	-	-	-	**3**	**1**	**1**	0.1	**3**
Pleurozium schreberi	-	-	-	-	-	-	-	-	0.1	0.1	0.1	-	-	-	-	-
Polytrichum juniperinum	-	-	5	-	-	-	-	-	0.1	-	**0.5**	-	-	-	-	-
Polytrichum strictum	-	-	0.1	-	-	-	-	-	2	-	-	-	-	-	-	-
Rhytidiadelphus subpinnatus	-	-	-	-	-	-	-	-	-	-	-	0.1	0.1	-	**0.5**	-
Sphagnum angustifolium	**68**	**61**	**46**	**15**	**15**	-	-	**4**	-	1	-	-	-	-	**24**	0.1
Sphagnum balticum	-	-	-	-	-	-	-	**4**	-	-	-	-	-	-	-	-
Sphagnum capillifolium	-	-	-	-	-	-	-	-	**68**	-	**95**	-	-	0.1	-	-
Sphagnum divinum	-	-	3	-	-	-	-	-	0.1	-	-	0.1	-	-	-	-
Sphagnum fallax	-	**10**	-	**35**	**30**	**18**	**5**	**58**	-	**40**	-	-	-	-	-	-
Sphagnum medium	0.1	-	**35**	-	-	-	-	-	-	-	-	-	-	-	-	-
Sphagnum papillosum	**4**	-	-	-	0.1	-	-	-	-	-	-	-	-	-	-	-
Sphagnum russowii	-	-	-	-	-	-	-	-	-	-	-	-	-	**91**	-	0.1
Sphagnum squarrosum	-	-	-	-	-	-	-	-	-	0.1	-	0.1	-	-	-	-
Sphagnum subsecundum	-	3	-	0.1	-	-	-	-	-	-	-	-	-	-	-	-
Sphagnum teres	-	-	-	-	-	**2**	**62**	-	-	**45**	-	-	-	-	0.1	**60**
Sphagnum wulfianum	-	-	-	-	-	-	-	-	0.1	-	-	-	-	-	0.1	-

Sphagnum warnstorfii	2	-	-	-	-	-	-	-	-	-	-	-	-	-	-	-
Warnstorfia spp.	-	-	-	0.1	-	0.1	3	0.1	-	-	-	-	-	-	-	-
Andromeda polifolia	7	**12**	11	4	8	-	5	3	0.1	-	-	-	-	-	-	-
Agrostis spp.	-	-	-	-	-	0.1	-	-	-	-	**0.5**	-	0.1	0.5	**15**	0.5
Betula nana	2	2	14	**5**	**14**	0.5	2	2	-	-	-	-	-	-	-	-
Betula pubescens	0.1	0.1	-	**5**	1	-	-	-	-	-	-	-	**5**	-	-	-
Calamagrostis spp.	-	-	-	-	-	-	-	-	-	-	-	**0.5**	-	-	-	-
Carex chordorrhiza	0.1	0.1	-	0.1	0.1	0.1	0.1	0.1	-	-	-	-	0.5	-	0.1	1
Carex echinata	0.5	-	-	0.1	0.1	0.1	-	0.1	**3**	**5**	-	**4**	**2**	**6**	5	4
Carex lasiocarpa	1	**7**	5	**22**	**13**	**15**	**7**	**12**	-	-	-	-	0.5	-	-	0.5
Carex limosa	0.1	-	-	-	-	-	-	-	-	-	-	-	-	-	-	-
Carex. livida	-	-	-	0.1	-	-	-	-	-	-	-	-	-	-	-	-
Carex pauciflora	0.5	0.1	0.1	-	-	-	-	0.1	0.1	0.5	0.1	0.1	-	0.1	-	-
Carex rostrata	1	0.5	-	3	2	0.5	2	1	-	-	-	-	-	-	-	-
Cirsium palustre	-	-	-	-	-	-	-	-	-	-	-	-	-	-	-	5
Dactylorhiza incarnata	-	0.5	-	-	-	-	-	-	-	-	-	-	-	-	-	-
Dactylorhiza maculata	2	-	-	-	-	-	-	-	-	-	-	-	-	-	-	-
Drosera longifolia	-	-	-	-	-	0.1	-	-	-	-	-	-	-	-	-	-
Drosera rotundifolia	0.5	0.1	-	0.1	-	0.1	0.5	0.1	-	-	-	0.1	-	0.1	0.1	0.1
Empetrum nigrum	-	-	-	-	-	-	-	-	-	-	0.1	-	-	-	-	-
Eriophorum angustifolium	-	-	-	-	0.5	2	-	-	0.5	2	**0.5**	-	-	-	-	-
Eriophorum vaginatum	-	-	0.1	0.1	-	-	-	-	-	-	0.1	-	-	-	-	-
Melampyrum spp.	-	-	-	-	-	-	-	-	0.5	-	-	-	-	-	-	-
Menyanthes trifoliata	**8**	0.5	6	-	-	-	-	-	-	-	-	-	-	-	-	-
Picea abies	0.1	0.1	-	-	-	-	-	-	-	-	-	-	-	-	-	-
Pinus sylvestris	2	4	**35**	2	0.5	-	0.1	0.1	0.5	1	0.1	**0.5**	0.1	-	-	0.1
Potentilla palustris	-	2	-	-	2	4	-	-	-	-	-	-	-	-	-	-
Scheuzeria palustris	0.5	0.1	-	0.1	0.5	-	0.1	0.1	-	-	-	-	-	-	-	-
Trichophorum alpinum	1	-	-	-	-	-	-	-	-	-	-	-	-	-	-	-
Trientalis europaea	-	1	-	-	-	-	-	-	-	-	-	**0.5**	-	**2**	**8**	**12**
Utricularia intermedia	-	-	-	-	-	4	-	-	-	-	-	-	-	-	-	-
Vaccynium ocycoccus	**11**	4	**20**	4	4	**5**	**7**	**7**	**2**	**3**	0.1	-	0.5	-	-	1
Viola palustris	-	0.1	-	-	-	4	-	-	-	-	-	-	0.1	0.1	0.1	**6**

S. fallax and *Sphagnum papillosum* were the most dominant bryophyte species at the oligotrophic control plot and were uniformly present in all but sample plot 5, where *Polytrichum strictum* and *Sphagnum warnstorfii* were dominant. Sample plot 5 was an outlier hummock that consistently had the lowest water table at the treatment plot. At the control plot *S. angustifolium* was the most dominant species, while *S. fallax* and *S. papillosum* were only intermittently present. *Aulacomium palustre* and *Sphagnum medium* also occurred on most plots at varying levels. *B. nana* had the most consistently high coverage among vascular plants

at the control plot. *A. polifolia*, *C. lasiocarpa*, *Pinus sylvestris*, *T. cespitosum* and *V. oxycoccos* were also present in most or all of the sample plots. *B. nana* and *V. oxycoccos* were the most dominant species at the WLD site, however *Empetrum nigrum* and *P. sylvestris* had the highest percentage covers recorded for vascular plants. *E. nigrum* was not present at the control plot. *T. cespitosum* and *C. lasiocarpa* were much less prevalent at the WLD plot than the control plot.

Table 3. Percentage cover of bryophytes (measured 23rd-29th September 2021) and vascular plants (measured 6th-13th July 2021) in **oligotrophic** sample plots. The two most abundant bryophytes and vascular plants are highlighted in bold.

Species	Control plots									WLD plots								
	1	2	3	4	5	6	7	8	9	1	2	3	4	5	6	7	8	9
Aulacomium palustre	-	0.1	-	0.1	0.5	-	0.2	0.2	5	0.1	-	**20**	**38**	1	0.5	0.1	0.1	**25**
Dicranum polysetum	-	-	-	-	-	0.5	-	-	-	-	-	-	-	-	-	-	-	-
Mylia anomala	-	-	-	-	-	-	-	-	-	-	-	-	-	-	0.1	-	-	-
Polytrichum juniperinum	-	-	-	-	-	-	-	-	-	-	5	**25**	-	0.1	14	-	**10**	-
Polytrichum strictum	-	0.5	-	-	**43**	0.5	-	-	-	-	-	-	-	0.1	-	-	-	-
Sphagnum angustifolium	8	2	2	**2**	-	**7**	1	6	4	**50**	**68**	**20**	**50**	**81**	**20**	**84**	**35**	**15**
Sphagnum divinum	-	-	-	-	-	-	-	-	-	-	-	-	-	-	-	-	2	-
Sphagnum fallax	**40**	**26**	**12**	**92**	-	**50**	**75**	**19**	**12**	-	-	-	-	0.5	**43**	-	-	-
Sphagnum medium	-	6	-	-	5	0.5	6	-	4	10	-	5	0.5	**11**	12	**0.5**	3	0.1
Sphagnum papillosum	**40**	**35**	**66**	0.5	-	3	**15**	**30**	**48**	**34**	**9**	-	-	-	-	-	-	-
Sphagnum warnstorfii	-	-	-	-	**38**	-	-	-	-	-	-	-	-	-	-	-	-	-
Andromeda polifolia	**6**	**4**	2	0.5	2	4	**4**	4	**7**	1	-	-	3	4	-	1	13	12
Betula nana	**10**	3	4	**4**	**11**	**7**	**7**	**14**	**13**	**18**	**15**	22	**24**	**12**	**23**	**20**	**15**	**27**
Betula pubescens	-	-	-	-	-	-	-	-	-	-	-	-	-	4	-	-	-	-
Carex lasiocarpa	3	2	2	**2**	1	0.5	2	0.1	0.5	-	-	-	-	-	-	-	0.5	-
Carex limosa	-	0.1	-	0.1	-	-	0.1	-	0.1	-	-	-	-	-	-	-	-	-
Carex magellanicum	-	-	-	-	-	-	-	-	-	-	-	-	-	-	-	-	5	8
Carex pauciflora	-	-	-	-	-	-	-	-	-	0.1	-	-	0.1	-	0.1	0.1	0.1	-
Carex rostrata	1	-	2	-	-	-	-	-	1	-	-	-	-	-	-	-	-	-
Drosera rotundifolia	2	1	0.1	0.5	-	-	0.1	-	-	0.1	-	-	0.1	0.5	-	-	-	-
Empetrum nigrum	-	-	-	-	-	-	-	-	-	-	**9**	**31**	-	**13**	-	-	-	-
Eriophorum angustifolium	-	0.5	-	-	-	-	-	-	-	-	-	-	-	-	-	-	-	-
Eriophorum vaginatum	1	0.1	2	**2**	-	1	2	12	0.1	2	2	0.5	0.5	3	-	3	1	2
Menyanthes trifoliata	-	0.5	**7**	-	-	-	-	-	-	-	-	-	-	-	-	-	-	-
Picea abies	-	-	-	-	-	-	-	-	-	**7**	-	-	-	-	-	-	-	-
Pinus sylvestris	0.1	**4**	**5**	**2**	**17**	1	0.1	3	1	0.5	5	**35**	**21**	4	8	-	4	-
Trichophorum alpinum	-	-	-	-	-	-	-	-	-	-	-	-	0.1	-	-	-	-	-
Trichophorum cespitosum	0.1	**16**	2	**2**	4	**21**	0.1	**18**	-	1	0.5	-	6	-	-	-	-	-
Vaccynium ocycoccus	1	2	0.5	1	2	2	2	4	5	1	1	1	20	10	**11**	**22**	**23**	**19**

No single bryophyte species was present across all of the ombrotrophic control sample plots. *Sphagnum balticum* was the most widespread, present in seven out of the ten sample plots. *Sphagnum fuscum* had the highest percentage coverages followed by *Sphagnum rubellum* and *S. balticum*. In plots 2 and 3, which could be characterised as hollows, *Sphagnum cuspidatum* was the only bryophyte species present. In the WLD plots *S. fuscum* was even more dominant, with over 90% cover in 3 plots and present in all others. *Sphagnum majus*, *S. angustifolium* and *S. rubellum* each had high percentage cover in several plots. *S. cuspidatum* was entirely absent from the WLD site. *E. vaginatum* was the most consistent presence in the ombrotrophic control plots. *A. polifolia, D. rotundifolia* and *V. oxycoccos* were present in almost all plots, though at fairly low levels. The most pronounced hollow plots (2 and 3) had less than 1% total vascular plant cover. At the WLD site, *E. vaginatum* was also the most dominant and widespread vascular plant species, occurring at higher levels than in the control plots. *A. polifolia, D. rotundifolia, P. sylvestris* and *V. oxycoccos* were also present in all of the plots. *E. nigrum* is notable for having high coverage in several plots and a much more substantial presence than at the control site.

Table 4. Percentage cover of bryophytes (measured 23rd-29th September 2021) and vascular plants (measured 6th-13th July 2021) in **ombrotrophic** plots. The 2 most abundant bryophytes and vascular plants are highlighted in bold.

Species	Control plots										WLD plots								
	1	2	3	4	5	6	7	8	9	10	1	2	3	4	5	6	7	8	9
Polytrichum juniperinum	-	-	-	-	-	-	-	-	-	-	-	-	-	-	-	-	0.5	-	-
Mylia anomala	-	-	-	-	-	-	-	-	-	-	0.1	0.1	-	-	-	-	0.1	0.1	-
Sphagnum angustifolium	-	-	-	-	-	-	-	-	-	2	**56**	**30**	-	-	**0.2**	1	0.2	**0.5**	0.5
S. balticum	1	-	-	1	2	-	**78**	3	0.1	**4**	8	-	-	-	-	-	-	-	-
S. cuspidatum	-	**16**	**3**	3	5	**4**	-	-	-	-	-	-	-	-	-	-	-	-	-
S. fuscum	**79**	-	-	**36**	**47**	-	-	**45**	**70**	**89**	4	**39**	**97**	4	**98**	**49**	**88**	**94**	1
S. majus	2	-	-	**45**	12	3	4	0.5	-	-	-	-	-	**10**	-	**20**	-	-	**84**
S. medium	-	-	-	5	**18**	-	-	-	-	-	**18**	-	-	-	-	-	0.5	**0.5**	-
S. rubellum	**15**	-	-	-	-	**79**	**15**	**40**	**29**	-	-	1	-	**61**	-	-	**4**	0.1	**7**
Andromeda polifolia	**3**	-	**0.1**	0.5	0.5	**0.5**	**2**	**5**	**3**	4	1	1	2	**2**	**2**	1	**7**	3	**3**
Carex pauciflora	-	-	**0.1**	-	-	-	-	-	-	-	-	-	-	-	-	-	-	-	-
Drosera longifolia	-	-	-	**1**	0.1	-	-	-	-	-	-	-	-	1	-	-	-	-	-
D. rotundifolia	**2**	**0.1**	-	0.5	**2**	0.1	0.1	1	0.5	0.5	0.1	0.1	0.5	0.5	0.1	**4**	0.1	1	0.1
Empetrum nigrum	0.1	-	-	-	-	-	-	0.1	2	**7**	**6**	-	**16**	-	**24**	-	2	5	**3**
Eriophorum vaginatum	1.5	**0.5**	**0.5**	**2**	**6**	**3**	**3**	**2**	1	2	2	**3**	**7**	**8**	**2**	**2**	**4**	**8**	**10**

Pinus sylvestris	0.1	-	-	-	-	0.1	-	0.5	0.1	0.1	2	0.1	1	0.1	0.5	0.1	0.5	0.5	0.5
Rubus chamaemorus	**2**	-	-	-	-	-	0.5	**2**	**8**	**5**	0.5	0.1	1	-	**2**	-	-	**8**	-
Trichophorum cespitosum	-	-	-	-	-	-	-	-	-	-	**12**	-	-	-	-	-	-	-	-
Vaccynium ocycoccus	0.1	**0.1**	-	0.1	0.5	0.1	0.5	0.5	0.1	0.1	0.5	**0.5**	0.1	0.5	0.1	0.5	1	0.1	0.5
V. uliginosum	-	-	-	-	-	-	-	-	-	4	2	-	-	-	1	-	-	-	-

Species richness was highest at the mesotrophic sites and lowest at the ombrotrophic sites, this was true for both bryophytes and vascular plants (Table 5). β diversity between control and WLD sites was greatest on the mesotrophic site and least for the ombrotrophic site. When considering only vascular plant species the oligotrophic site had a similar species turnover to the mesotrophic site.

Table 5. Plant species richness of the study sites and Whittaker's β diversity (β_w) between respective control and WLD sites. $\beta_w = \frac{total\ species\ pool}{average\ site\ species\ richness} - 1$

Site	Species richness						Whittaker's β diversity (2 sig. fig.)		
	Bryophytes		Vascular plants		Total plants		Bryophytes	Vascular plants	Total plants
Meso control	13	21	27	31	40	52	0.5	0.38	0.42
Meso WLD	15		18		33				
Oligo control	8	11	12	18	20	29	0.29	0.38	0.35
Oligo WLD	9		14		23				
Ombro control	7	9	10	11	17	20	0.2	0.1	0.14
Ombro WLD	8		10		18				

The same pattern of differences in community composition are reflected in the DCA (Figure 15). The largest difference between WLD and control plots within sites is found at mesotrophic site, followed by the oligotrophic site, while in the ombrotrophic site the WLD impact is less distinguishable. The first axis (DCA1) broadly reflects nutrient status, as seen from the clear gradient between the different sites. However, the differences between the mesotrophic control and WLD sites on this axis may represent both increased nutrient availability and increased shading. The second axis (DCA2) appears to reflect microtopographical differences, with the ombrotrophic and mesotrophic sites showing the greatest variation. The more negative values are seen in hollow species, e.g., *S. cuspidatum* and *Drosera longifolia*, while hummock species occur at positive values, e.g., *S. fuscum*, *V. uliginosum* and *E nigrum*.

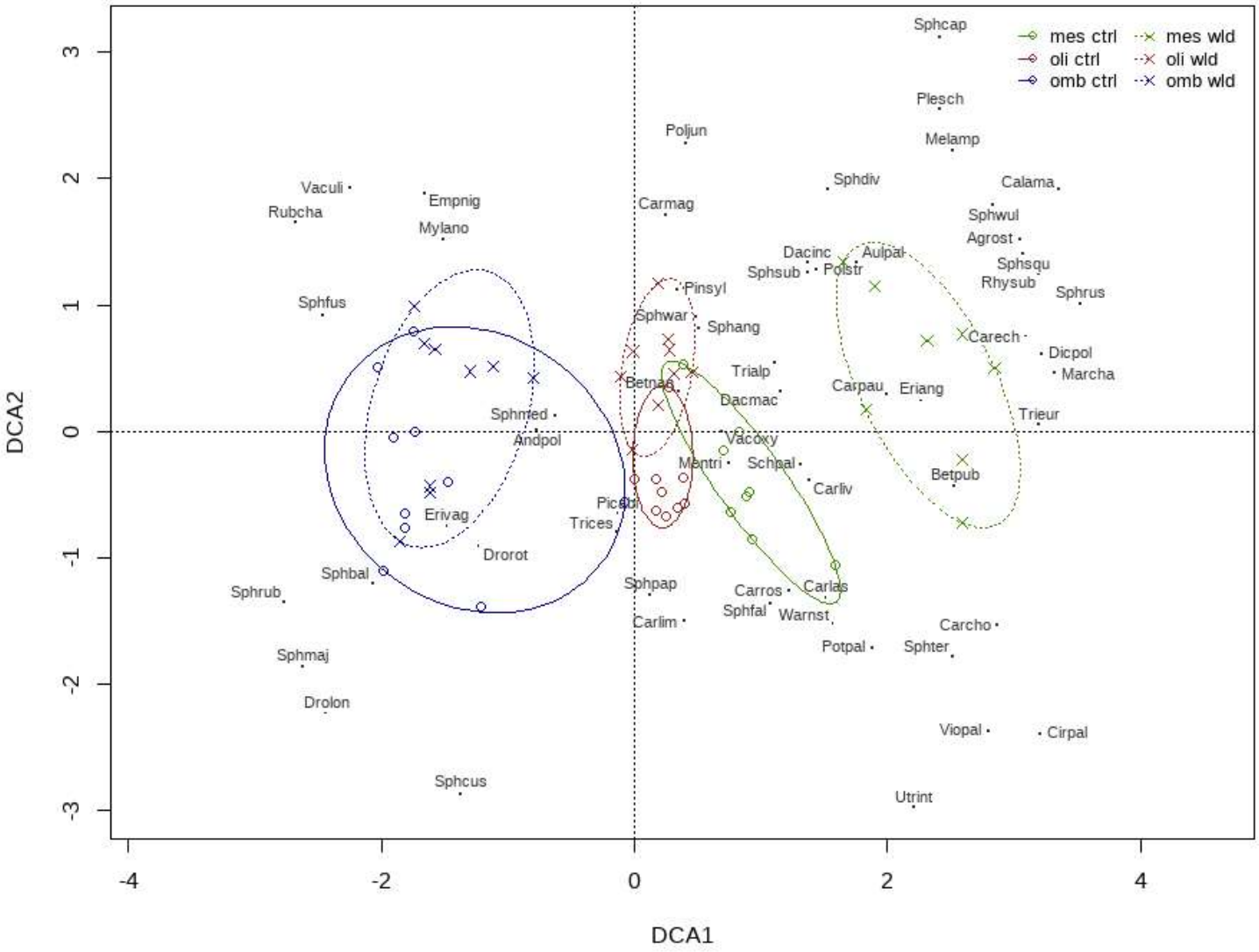

Figure 15. Detrended correspondence analysis (DCA) based on plant community percentage cover. Bryophytes were measured 23rd-29th September 2021 and vascular plants were measured 6th-13th July 2021. Species are marked in the plot using the first 3 letters of both the generic and specific names, for a translated list see Appendix 3. The eigenvalue for DCA1 is 0.6683 and for DCA2 it is 0.3212.

3. 3 Impact of WLD on LAI development

Site, WLD treatment and year interacted in their effects on the seasonal course of LAI development (Table 6). WLD had a significant negative effect on LAIMAX in both years at the mesotrophic site (p<0.0001 and p=0.0008 respectively). Differences were not significant at the other two sites, however, for both sites WLD resulted in lower LAIMAX in 2017 and more in 2021 (Figure 16). Relative to 2017, the warmer year 2021 (Figure 9) uniformly resulted in

greater LAIMAX across all sites and their treatments (Figure 17). However, this effect of year was significant only for WLD treatment plot and none of the control plots. As such there was a significant interaction between the effect of year and WLD (p=0.0003).

Table 6. Log transformed parameter estimates for leaf area maximum (LAIMAX), timing of LAIMAX (DMAX) and Shape, which represents a non-unit measure of the width of the growing season. For all parameters the intercept is the mesotrophic control site in 2017 (mesocontrol2017) to which all other sites, WLD treatment and year 2021 are compared. The pairwise comparisons between the levels of explanatory variables are reported in Appendix 1. DMAX values are days since Julian date 110, set as the start of the growing season. The random effects included in the model are displayed at bottom.

Fixed predictors	Value	Std. error	t-value	p-value
LAIMAX (m^2 m^{-2})				
Intercept (mesocontrol2017)	-0.07305	0.119009	-0.61383	0.5396
2021	0.190205	0.124048	1.53331	0.1259
Wld	-1.57452	0.216795	-7.26273	<0.0001
Oligo	-0.51591	0.143507	-3.59497	0.0004
Ombro	-1.34136	0.159384	-8.41588	<0.0001
2021*wld	0.700224	0.191992	3.64716	0.0003
wld*oligo	1.256472	0.234101	5.36723	<0.0001
wld*ombro	1.203493	0.258516	4.65538	<0.0001
DMAX (Julian date)				
Intercept (mesocontrol2017)	4.534273	0.024003	188.9036	<0.0001
2021	-0.22375	0.039138	-5.71702	<0.0001
Wld	-0.1063	0.037084	-2.86633	0.0043
Oligo	-0.08282	0.038905	-2.12871	0.0338
Ombro	0.045208	0.083158	0.54364	0.5870
2021*oligo	0.238301	0.059695	3.992	0.0001
2021*ombro	0.135901	0.099021	1.37245	0.1706
Shape				
Intercept (mesocontrol2017)	-0.67659	0.057401	-11.787	<0.0001
2021	0.277202	0.084881	3.26579	0.0012
Wld	-0.52422	0.327372	-1.60131	0.1100
Oligo	-0.18168	0.095811	-1.89625	0.0586
Ombro	0.208117	0.203931	1.02053	0.3080
2021*wld	-0.23653	0.346784	-0.68208	0.4955
2021*oligo	0.382429	0.144746	2.64207	0.0085
2021*ombro	-0.38525	0.266184	-1.4473	0.1485

wld*oligo	1.164304	0.360367	3.23088	0.0013
wld*ombro	0.368566	0.425784	0.86562	0.3872
2021*wld*oligo	-0.71759	0.388471	-1.84723	0.0654
2021*wld*ombro	0.20892	0.480613	0.4347	0.6640
Random part	StDev			
LAIMAX (m^2 m^{-2})				
$\sigma(b_p)$	0.3849			
$\sigma(e_{pm})$	0.1370			

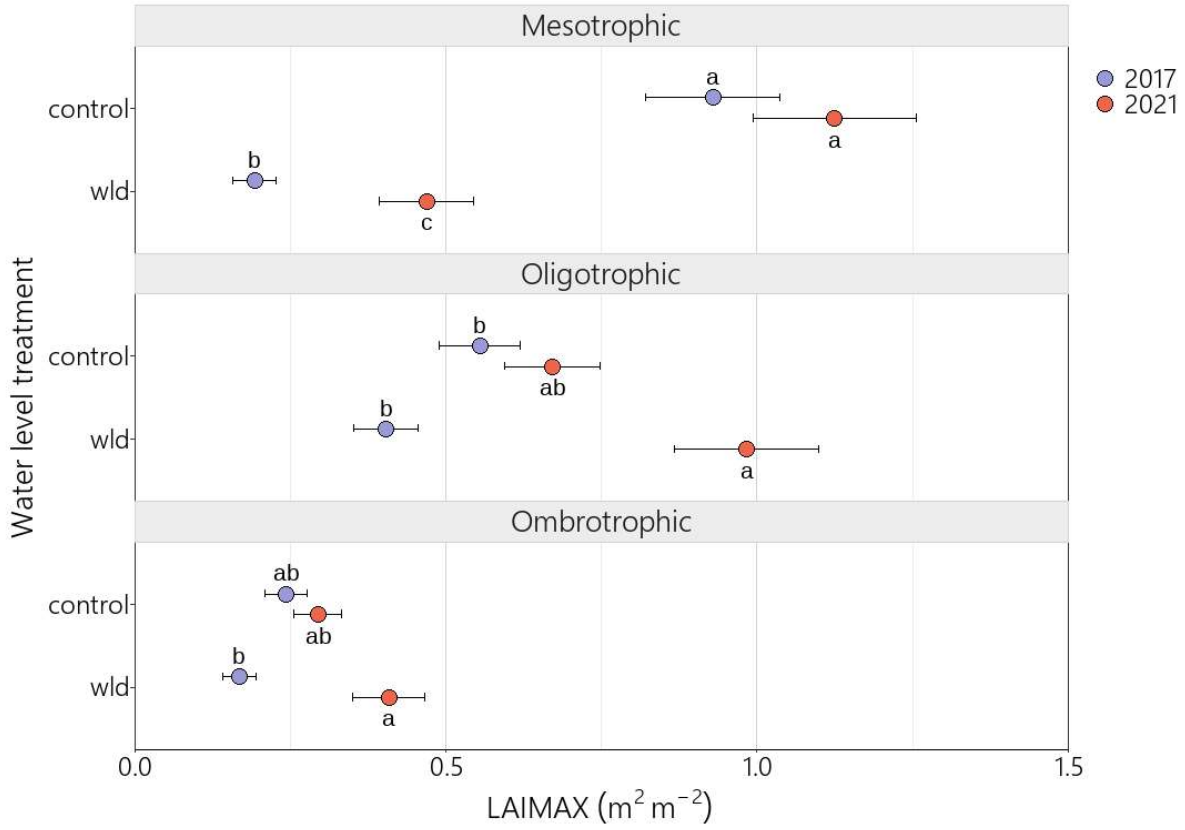

Figure 16. Model estimates and standard error for LAIMAX, results are back-transformed to the original scale. Letters indicate significance groupings within nutrient levels only.

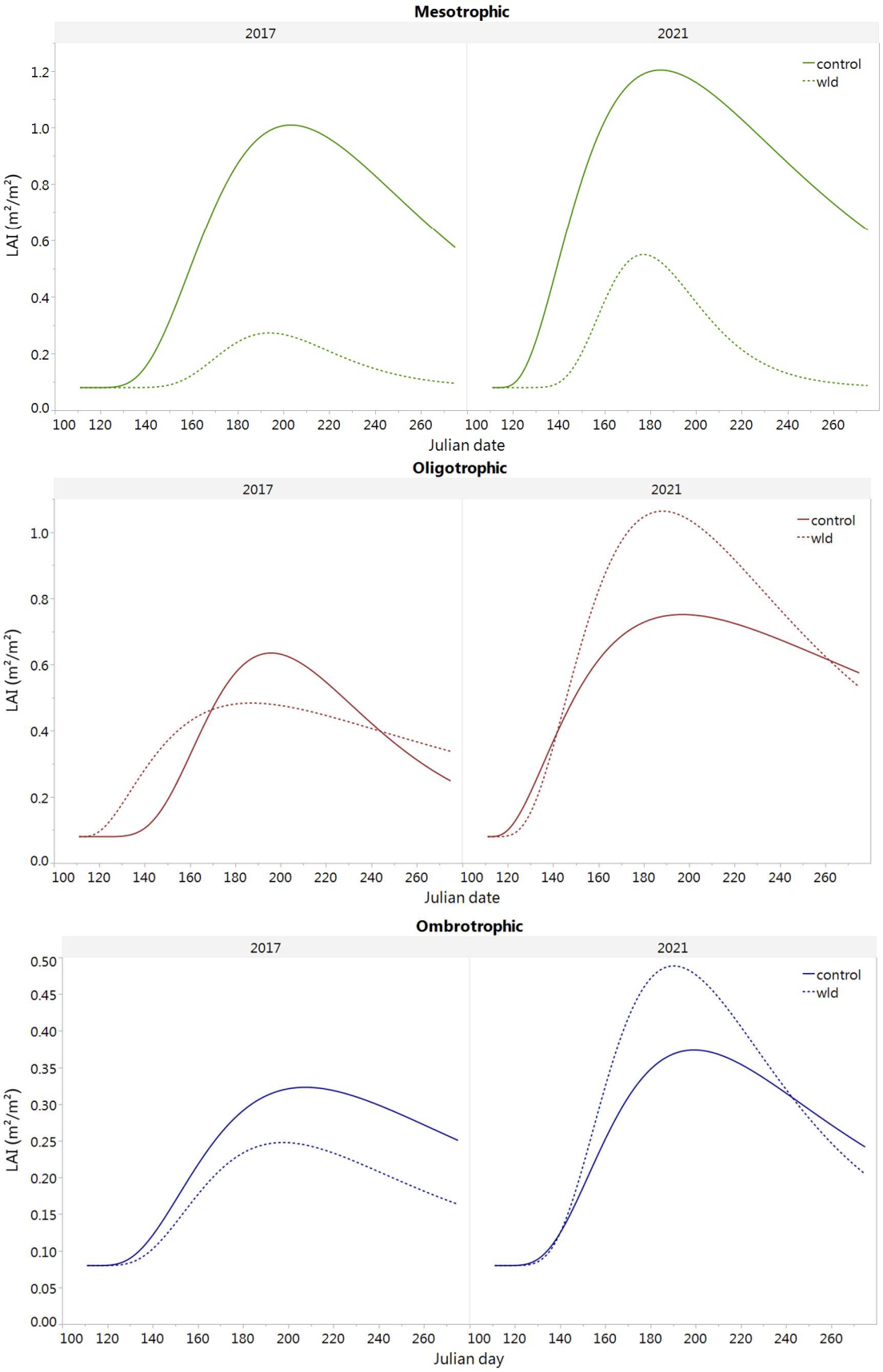

Figure 17. Phenological response of LAI (m^2 m^{-2}) over the course of the season reconstructed using the model's parameter estimates.

2021 resulted in significantly earlier DMAX at the mesotrophic site, more than 15 days for both the control and WLD plots (p<0.0001 for both) (Figure 18). The effect was not significant for either of the other sites though the ombrotrophic site suggested the same pattern. Overall, WLD resulted in significantly earlier DMAX (p=0.0043), by an average of 9 days, but there were no significant differences between any of the pairwise comparisons (Appendix 1b).

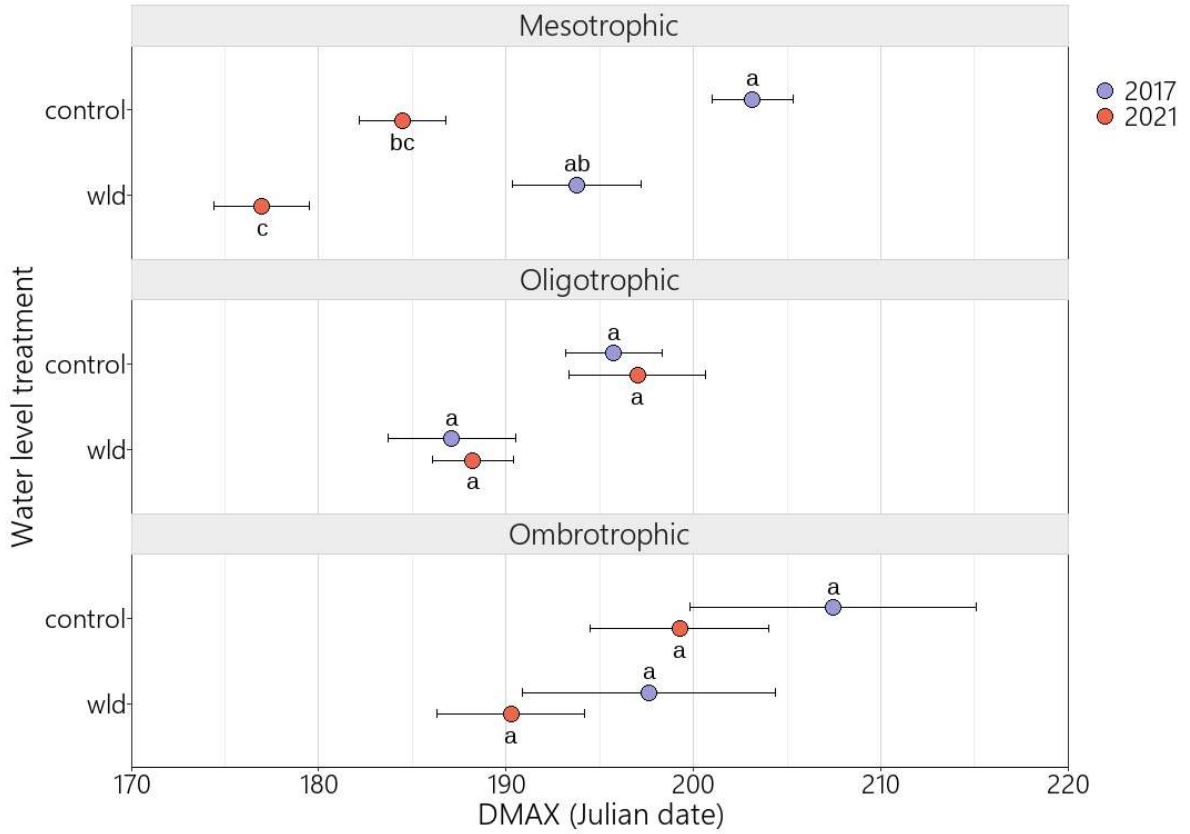

Figure 18. Model estimates and standard error for DMAX, results are back-transformed to the original scale. Letters indicate significance groupings within nutrient levels only. Julian dates: 91 = 1st April; 121 = 1st May; 152 = 1st June; 182 = 1st July; 213 = 1st August; 244 = 1st September.

Overall, year had a mixed effect on the Shape of the growing season (Figure 19). Year 2021 resulted in significantly lengthened growing seasons for the mesotrophic and oligotrophic controls as indicated by higher Shape parameter value and less sharp LAI development (p=0.0418 and p<0.0001 respectively). However, the oligotrophic WLD and both ombrotrophic plots had narrower growing seasons in 2021, though these differences were not significant (Figure 19). WLD also had inconsistent effects on Shape. At the mesotrophic site, the WLD plot had a lower Shape value, i.e., narrower period with high LAI, though the difference was only significant in the warmer year of 2021 (p<0.0001). In contrast, in the cooler

year 2017, the oligotrophic WLD site had a significantly higher Shape value, i.e., broader period with high LAI (or longer growing season), than the control site (p=0.0020). This difference between the oligotrophic site treatments appears reversed in 2021, though the difference is not significant (p=0.0884). As such, the interaction between the year and WLD treatment was highly significant for the oligotrophic site (p<0.0001). No differences were evident at the ombrotrophic site and there were no interactions between year and WLD treatment at either the mesotrophic or ombrotrophic sites. There was a significant 3-way interaction effect between the oligotrophic and ombrotrophic sites and the effects of WLD and year (p=0.0170). No other 3-way interactions were significant.

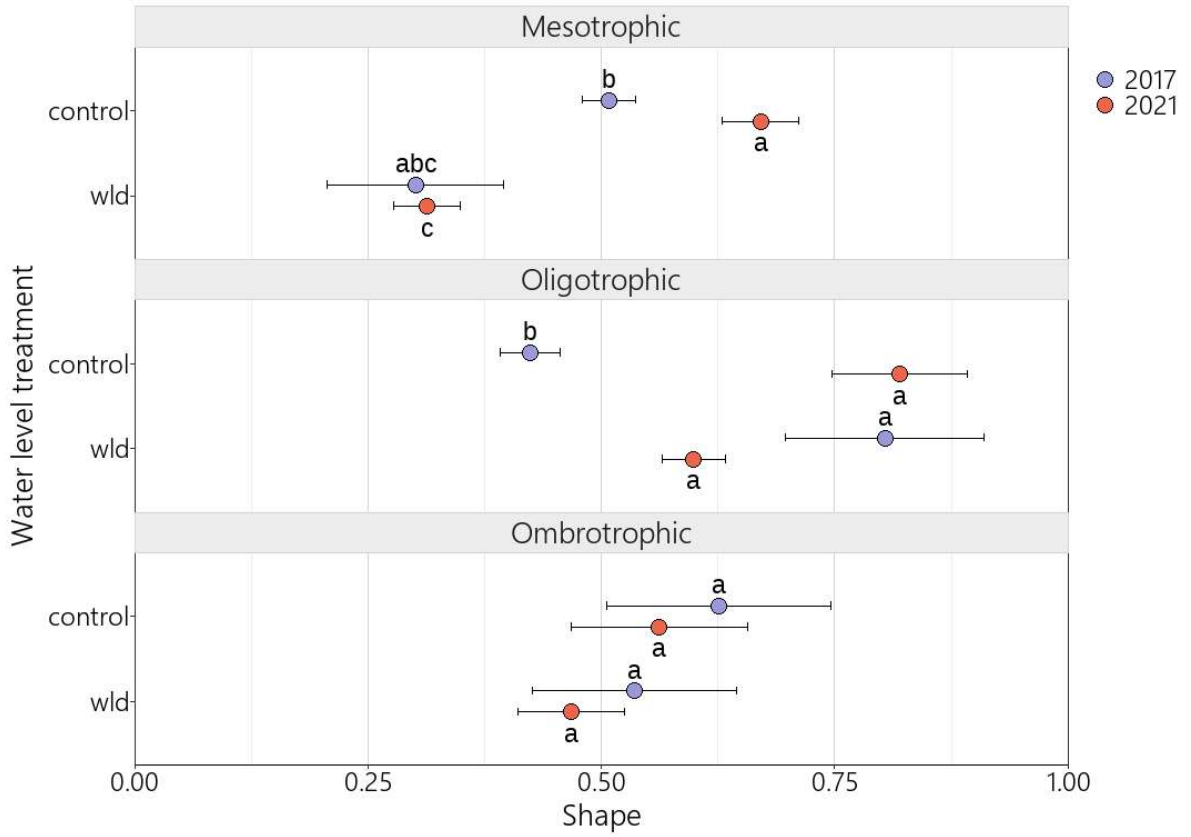

Figure 19. Model estimates and standard error for Shape, results are back-transformed to the original scale. Letters indicate significance groupings within nutrient levels only.

4 DISCUSSION

4.1 Comparability of results

The values for leaf area phenology recorded here are broadly within the range of previously reported values from northern peatlands using the same methods. LAIMAX equivalent values range from 0.3 $m^2 m^{-2}$ at an Alaskan fen to as high as 1.5 $m^2 m^{-2}$ for certain microtopographical features of an Irish bog and 5 $m^2 m^{-2}$ at a Czech fen site (Chivers et al. 2009, Laine et al. 2007, Urbanova et al. 2012). Given the differences in climate and site character, few of these studies are directly comparable. However, there are also several studies including Finnish sites of similar character.

Leppälä et al. (2011) studied various mire types in coastal western Finland. LAIMAX values at the mesotrophic fen site were approximately 1.8 - 2.5 $m^2 m^{-2}$, around 0.8 $m^2 m^{-2}$ at the oligotrophic site and ranged from 1 - 1.3 $m^2 m^{-2}$ across microtopography at a bog site. Regarding the higher figures for the bog site, it is worth remembering that hollows, which have the least vascular plant growth of the ombrotrophic microtopographical types, were not included in Leppälä et al. (2011).

Mäkiranta et al. (2018) recorded LAIMAX values between 0.8 - 1.2 $m^2 m^{-2}$ at Lakkasuo in 2011 and 2012, at a study site similar to the oligotrophic site in this study. For comparison the LAIMAX means for the oligotrophic control plot from this study were 0.55 $m^2 m^{-2}$ in 2017 and 0.67 $m^2 m^{-2}$ in 2021. DMAX values in Mäkiranta et al (2018) were around DOY 190, the values for the oligotrophic site in this study were 196 in year 2017 and 197 in year 2021. So overall the results from this study are both later and lower, but not entirely dissimilar. The differences may reflect the character of the plots used.

It is most notable that Wilson et al. (2007) found markedly higher LAIMAX values across the mire types at Lakkasuo in 2002 and 2003. LAIMAX values they recorded were 1.6 - 3.3 $m^2 m^{-2}$ for the mesotrophic site; 0.6 - 1.9 $m^2 m^{-2}$ for the oligotrophic site and 0.5 – 1 $m^2 m^{-2}$ for the ombrotrophic site. The values for the oligotrophic site reported in this study are lower but within the same range. However, the mesotrophic and ombrotrophic LAIMAX means were substantially lower than those in Wilson et al. (2007), 0.93 $m^2 m^{-2}$ in 2017 and 1.12 $m^2 m^{-2}$ in 2021 for the mesotrophic control plot and 0.24 $m^2 m^{-2}$ in 2017 and 0.29 $m^2 m^{-2}$ in 2021 for the ombrotrophic control plot. There is a slight difference in methodology, since Wilson et al. (2007) uses species specific coefficients to describe leaf shapes which may record slightly

higher values relative to the method used here. Additionally, the ombrotrophic plots in Wilson et al. (2007) are lawn level vegetation, whereas in this study they are a mix of lawn, hummock and hollow microtopography. Hollow areas have far less vascular plant cover than lawn or hummocks and as such their inclusion reduces the overall mean values.

A more intriguing possibility is that these results may represent a long term decrease in productivity at the mesotrophic site, since the Wilson et al. (2007) measurements were conducted in 2002 and 2003. This may relate to changes in the ecohydrological regime. However, further work would be needed to establish this. The timing of DMAX in Wilson et al. (2007) is fairly uniform in occurring in early July across the sites. The DMAX was more variable in this study, however mean DMAX was within July for all control plots in both years.

4.2 Impact of WLD on leaf area and community composition

Overall WLD had a variable effect on the seasonal development of vascular plant leaf area, depending on both study site and measurement year. However, WLD resulted in significantly earlier seasonal growth peaks, this being the one unequivocal effect of WLD across the study. It is notable that in contrast, Mäkiranta et al. (2018) found no changes in DMAX as a result of WLD. However, the drying effect employed in that study was lesser in magnitude and duration. 3 - 7 cm WLD for 4-5 years compared with 15 cm WLD for 16-20 years in the current study. There are no clear differences in community composition between control and WLD plots that occur across all sites which would explain this pattern. Neither is the earlier DMAX explained by early senescence in response mid-season drought stress, in which an early die-off of vascular plants, particularly sedges, would skew the growth peak earlier (Bubier et al. 2003). If this were the case, we would expect the difference between the timing of DMAX at control and WLD plots to be greater during the dry year 2021. One possible explanation is that drier soils are facilitating earlier warming of the soil, due to decreased specific heat capacity, allowing earlier and faster plant growth. It has been demonstrated that drainage can result in warmer soils and earlier phenological responses on peatlands (Lieffers and Rothwell 1987). However, over the long term, shading induced by increased tree growth at drained sites results in an overall negative impact on peat temperatures (Laiho 2006, Straková et al. 2012). Shading is increased at both the mesotrophic and oligotrophic WLD plots relative to their control plots due to greater tree growth, suggesting this warming explanation is unlikely to hold across all the sites.

At the mesotrophic site, the community compositional differences may explain the earlier DMAX in response to WLD. Mäkiranta et al. (2018) observed the difference in DMAX between plant functional groups; evergreen shrubs peak later than the others. At the mesotrophic control plot evergreen shrubs represent 46% of total vascular plant cover, predominately *A. polifolia* and *V. oxycoccos*, while at the WLD plot their share in the understorey vegetation is reduced to 9%. Percentage cover is not an exact corollary with leaf area; however, it is certain that evergreen shrubs have a diminished presence at the WLD plot which may explain the earlier DMAX.

WLD also had a significant suppressive effect on LAIMAX at the mesotrophic site. Underlying this is a wholesale change in the community composition. The mesotrophic site had the highest β diversity between the control and WLD treatment plots. This change represents a shift at the WLD plot towards a new regime, dominated by forest associated species. Kokkonen et al. (2019) identified these changes up to 2016 and noted that community had not yet stabilised. The current study suggests that compositional changes in the mesotrophic WLD plot have continued, and since 2016, new forest associated species have arrived (e.g., *Marchantiophyta spp, R. subpinnatus, Sphagnum squarrosum* and *Melampyrum spp*). Changes in community composition are both a response to changing abiotic conditions directly resulting from a lowered water table and a response to changes resulting from biotic mediators, e.g. increased shading from tree encroachment and increased nutrient cycling due to enhanced aerobic microbial activity. Therefore, when considering the effect of WLD on the seasonal leaf area development it is a complex task to disentangle the direct effects of WLD, the effects of secondary changes, particularly shading, and altered species composition, and it is beyond the scope of this study to do so.

The effects of WLD on the seasonal leaf area development at the oligotrophic site were equivocal. However, community compositional differences were more profound and vascular plant species turnover between the control and WLD treatment plots was as high as at the mesotrophic site (Table 5). Additionally, there has been a clear shift in the dominance of functional groups, with increased evergreen and deciduous shrubs presence at the WLD treatment plot and less sedges and forbs relative to the control treatment plot. It is also not obvious how the community compositional changes may explain the oligotrophic portion of the overall pattern of earlier DMAX in response to WLD, since here evergreen shrubs represent a greater proportion of vascular vegetation at the WLD plot. However, it is worth noting that the oligotrophic WLD treatment plot has experienced less tree encroachment and consequently

is not as shaded as the mesotrophic WLD plot (based on field observation). So, increased soil warming in response to drying remains a possible explanation.

The ombrotrophic site showed the least response in leaf area phenology to WLD. There were no significant differences in control and WLD pairwise comparisons for any phenological parameters. While difference in the water table was least apparent at this site, ombrotrophic sites have been observed previously to maintain continuity in water level through negative feedback mechanisms (Bridgham et al. 2008). The lack of change is also underpinned by the relative lack of community compositional changes, ombrotrophic treatment plots have diverged the least of all the sites. The small shifts towards decreased presence of hollow species at the WLD plot (e.g., *S. cuspidatum* and *S. balticum*) and increases in hummock species (e.g., *E. nigrum* and *S. fuscum*) are broadly in line with the direction of changes observed in Kokkonen et al. (2019) and in palaeoecological evidence (Väliranta et al. 2007, Zhang et al. 2020). The overall increase in vascular plant coverage at the WLD treatment plot, most notably sedges and evergreen shrubs, likely reflects the relative paucity of vascular plants in the bog hollows.

4.3 Sensitivity of leaf area development to growing season weather

Warmer, drier growing conditions in 2021, led to increased LAIMAX across all sites, though not all pairwise comparisons were significant. It is necessary to be cautious in interpreting the effect of the meteorology on the leaf area development, as there is a four-year interval between the two years included in this study, in which successional processes have altered species composition of the treatment plots and at unequal rates. Nonetheless, the meteorological results clearly show the difference between the years 2017 and 2021. In 2021 temperatures were higher and the growing season both started earlier and accumulated more heat units. However, the greater evapotranspirative demand and relative scarcity of rainfall in the middle of the summer also created a dry period. It is worth remembering that the water balance model used is simple and only considers precipitation and PET. This ignores the role of lateral inputs and outputs, which by definition differ between the study sites. Nonetheless, the actual water table data demonstrates the extent of the ‘drought’ effect at each of the sites. However, it seems that the warmer temperatures had a greater positive effect on LAIMAX than any drought stress. This runs counter to the findings in Leppälä et al. (2011) who found no significant differences in

LAIMAX between a warmer dry year and a cooler wet year across a range of comparable mires. However, the temperature difference between the years in this study was greater, there was 30% less GDD in the cooler year, than in Leppälä et al. (2011), in which there was only an 8% reduction in GDD in the cooler year. The drought effect was also more pronounced in that study with growing season precipitation in the drier year less than half that of the wetter year. In the current study, despite the mid-summer drought period in 2021, total growing season precipitation volume was similar between the two years. Additionally, the sites studied in Leppälä et al. (2011) are younger and consequently have a shallower peat layer, making them more susceptible to drought. Consequently, the lack of difference observed in Leppälä et al. (2011) may result from the drought effect and warming effect cancelling each other. Alternately, peatland plants may be largely buffered against moderate drought conditions and the lack of difference in Leppälä et al. (2011) is due to the smaller temperature difference between the years observed in that study.

In these circumstances we might also expect an earlier peak season in the warmer dryer year, as warmer spring temperatures favour rapid growth while mid-season drought may cause early senescence (Bubier et al. 2003). In accordance with this, the seasonal leaf area peak at the mesotrophic site occurred significantly earlier in 2021 than in 2017. However, there were no significant differences in DMAX between the two years at the oligotrophic and ombrotrophic sites. It is important to note that in this study there were only single replicates for each treatment plot owing to resource constraints, which is a frequent challenge in studies involving significant ecosystem modification. Consequently, it is necessary to use and interpret inferential statistics with caution, since this constitutes pseudoreplication (Hurlbert 1984). Nonetheless, sensible ecological interpretation regarding the effects of drying on different mire types is possible and the data here supports existing evidence suggesting mesic peatlands are less stable in the face of environmental change (Bubier et al. 2003, Oksanen 2004, Davies and Gray 2015).

4.4 Interactions between growing season weather and WLD in the control of leaf area development

Across all the study sites, WLD plots had a significantly larger LAIMAX in the warmer year 2021 than in 2017, while the difference between the years was not significant at control sites. This interaction between the effects of long-term drying and yearly weather on LAIMAX is principal result of the study. There are several potential explanations for this. WLD treatment

has in most cases favoured more drought-tolerant plant species, that are then better able to take advantage of the warm dry conditions in 2021. Overall, sedges are expected to be more vulnerable to drought stress and shrub species to be less so (Bubier et al. 2003), and overall shifts in this direction have occurred across the study sites. Though equally we might expect WLD sites to be more affected by dry conditions since the drought-induced drop in water level is more pronounced there (Figure 12). Overall, it seems that drought effect is not a major factor in the dynamics seen in this study. This may reflect the fact that the dry period in year 2021 only occurs from July onwards. Inevitably the effect of weather events on plant functioning and phenology is dependent on timing (Lund et al. 2012, Peichl et al. 2018). Griffis et al. (2000) suggests that drought during the spring leads to depressed growth, however, after that initial growth period drought-vulnerable vascular plants are likely to have already established deeper root systems. Nonetheless there is a clear pattern suggesting that WLD results in lower stability of the mire ecosystems in response to weather conditions.

The warmer year 2021 resulted in significantly greater scale values for the mesotrophic and oligotrophic control plots, meaning they had longer 'green' seasons relative to 2017. These plots are both sedge-dominated. While the study plots that might be characterised as pine, shrub and *Sphagnum* dominated, the oligotrophic WLD and both ombrotrophic plots, had 'narrower' seasons in 2021 relative to 2017, though the differences here were not significant. This raises the possibility that sedges are plastic in their phenological strategy in terms of extending the green season, even if seasonal maximum leaf area may be limited by other factors, such as conditions during the previous season.

4.5 Implications

Overall, the differential response at the study sites in seasonal leaf area development and community composition seem to support the existing body of research that more nutrient rich peatland sites are likely to be both less stable and less resilient in the face of climate change (Bridgham et al. 1999, Bubier et al. 2003, Adkinson et al. 2011). While this runs counter to established theories about the relationship between species diversity and ecosystem resilience, it highlights that in some ecosystems underlying structural drivers play a more significant role (Hector et al. 1999, Steudel et al. 2012). In the case of peatlands, the various feedback mechanisms associated with ombrotrophic systems are likely a major source of resilience and

stability, maintaining the system within current boundaries (van Breemen 1995, Granath et al. 2010, Waddington et al. 2015). It remains to be seen if larger climatic shifts would be sufficient to exceed these limits and substantially alter the structure of ombrotrophic mires (Frankl and Schmeidl 2000, Gunderson 2000).

The interactive effect observed here, where the WLD plots responded more strongly to meteorological variation, suggests long-term baseline shifts in climate may make peatland ecosystem functioning more vulnerable to extreme events. This response will only be compounded by the increasing interannual variation and likelihood of extreme events in the future climate (Füssel et al. 2017). The implications are particularly notable in relation to carbon cycling. Leaf area phenology is the principal driver of primary production on peatlands (Peichl et al. 2015, Koebsch et al. 2019), as such, we can expect climate driven drying to affect the ability of peatlands to remain consistent carbon sinks. In drought years peatlands can switch to become carbon sources, as falling water tables drive increases in aerobic respiration and limit the ability of plants to photosynthesise (Griffis et al. 2000, Lund et al. 2012, Peichl et al. 2014, Rinne et al. 2020). There was no clear sign of drought reducing seasonal growth peaks or season length in this study. However, it has been shown that the relationship between phenology and primary productivity can weaken during drought periods (Peichl et al. 2018). Bryophytes are more sensitive to water level, and as such, measures of greenness may be more appropriate than leaf area when considering phenology in relation to drought impacts as a driver of CO_2 fluxes (Riutta et al. 2007). It is also likely that vascular plants first rely on physiological mechanisms to control water loss through photosynthesis, such as stomatal closure and reduced enzyme activity, and costly structural responses like leaf shedding and early senescence are a last resort used in the most extreme conditions.

5 CONCLUSION

To summarise, climate driven long-term drying has the potential to substantially alter the composition and phenology of northern peatlands. This has complex implications for their continued role as net sinks in the global carbon cycle. Low nutrient peatlands exhibit the most resistance to these changes. However, this study provides evidence that long-term drying may reduce the stability of peatland functioning in response to interannual variation in weather, with the effects still evident on poorer peatlands, though to a lesser extent. This interaction suggests

an increased level of complexity may be required in modelling future carbon flux dynamics on peatlands. Further study is necessary to better resolve the species level shifts underpinning these functional changes.

6 REFERENCES

Adkinson, A. C., Syed, K. H., & Flanagan, L. B. (2011). Contrasting responses of growing season ecosystem CO2 exchange to variation in temperature and water table depth in two peatlands in northern Alberta, Canada. Journal of Geophysical Research: Biogeosciences, 116(G1), n/a. https://doi.org/10.1029/2010JG001512

Ahti, T., Hämet-Ahti, L., & Jalas, J. (1968). Vegetation zones and their sections in northwestern Europe. Annales Botanici Fennici,

Bridgham, S. D., Pastor, J., Dewey, B., Weltzin, J. F., & Updegraff, K. (2008). Rapid Carbon Response of Peatlands to Climate Change. Ecology (Durham); Ecology, 89(11), 3041-3048. https://doi.org/10.1890/08-0279.1

Bridgham, S. D., Pastor, J., Updegraff, K., Malterer, T. J., Johnson, K., Harth, C., & Chen, J. (1999). Ecosystem control over temperature and energy flux in northern peatlands. Ecological Applications, 9(4), 1345-1358.

Bubier, J. L., Bhatia, G., Moore, T. R., Roulet, N. T., & Lafleur, P. M. (2003). Spatial and temporal variability in growing-season net ecosystem carbon dioxide exchange at a large peatland in Ontario, Canada. Ecosystems, 353-367.

Chivers, M. R., Turetsky, M. R., Waddington, J. M., Harden, J. W., & McGuire, A. D. (2009). Effects of Experimental Water Table and Temperature Manipulations on Ecosystem CO_2 Fluxes in an Alaskan Rich Fen. Ecosystems (New York), 12(8), 1329-1342. https://doi.org/10.1007/s10021-009-9292-y

Couwenberg, J., Thiele, A., Tanneberger, F., Augustin, J., Bärisch, S., Dubovik, D., Liashchynskaya, N., Michaelis, D., Minke, M., Skuratovich, A., & Joosten, H. (2011). Assessing greenhouse gas emissions from peatlands using vegetation as a proxy. Hydrobiologia, 674(1), 67-89. https://doi.org/10.1007/s10750-011-0729-x

Davies, G. M., & Gray, A. (2015). Don't let spurious accusations of pseudoreplication limit our ability to learn from natural experiments (and other messy kinds of ecological monitoring). Ecology and evolution, 5(22), 5295-5304. https://doi.org/10.1002/ece3.1782

Dorrepaal, E., Toet, S., van Logtestijn, R. S. P., Swart, E., van de Weg, M. J., Callaghan, T. V., & Aerts, R. (2009). Carbon respiration from subsurface peat accelerated by climate warming in the subarctic. Nature (London), 460(7255), 616-619. https://doi.org/10.1038/nature08216

Frankl, R., & Schmeidl, H. (2000). Vegetation change in a South German raised bog: Ecosystem engineering by plant species, vegetation switch or ecosystem level feedback mechanisms? Flora, 195(3), 267-276.

Frolking, S., Roulet, N., & Fuglestvedt, J. (2006). How northern peatlands influence the Earth's radiative budget: Sustained methane emission versus sustained carbon sequestration. Journal of Geophysical Research - Biogeosciences, 111, G01008-n/a. https://doi.org/10.1029/2005JG000091

Füssel, H., Jol, A, Marx, A, Hilden, M. (2017). Climate change, impacts and vulnerability in Europe 2016: an indicator-based report. P. Office.

Granath, G., Strengbom, J., & Rydin, H. (2010). Rapid ecosystem shifts in peatlands: linking plant physiology and succession. Ecology, 91(10), 3047-3056.

Green, S., & Baird, A. (2012). A mesocosm study of the role of the sedge Eriophorum angustifolium in the efflux of methane—including that due to episodic ebullition—from peatlands. Plant and soil, 351(1), 207-218. https://doi.org/10.1007/s11104-011-0945-1

Griffis, T. J., Rouse, W., & Waddington, J. (2000). Interannual variability of net ecosystem CO2 exchange at a subarctic fen. Global Biogeochemical Cycles, 14(4), 1109-1121.

Gunderson, L. H. (2000). Ecological resilience—in theory and application. Annual review of ecology and systematics, 31(1), 425-439.

Hector, A., Schmid, B., Beierkuhnlein, C., Caldeira, M., Diemer, M., Dimitrakopoulos, P. G., Finn, J., Freitas, H., Giller, P., & Good, J. (1999). Plant diversity and productivity experiments in European grasslands. science, 286(5442), 1123-1127.

Helbig, M., Waddington, J. M., Alekseychik, P., Amiro, B. D., Aurela, M., Barr, A. G., Black, T. A., Blanken, P. D., Carey, S. K., & Chen, J. (2020). Increasing contribution of peatlands to boreal evapotranspiration in a warming climate. Nature Climate Change, 10(6), 555-560.

Hurlbert, S. H. (1984). Pseudoreplication and the Design of Ecological Field Experiments. Ecological Monographs, 54(2), 187-211. https://doi.org/10.2307/1942661

ICOS. (2018). ICOS Ecosystem Station Labelling Report: Hyytiälä Station. ICOS. https://data.icos-cp.eu/objects/V1dIG1MK5wm_Hj5FUMmPD72T

Koebsch, F., Sonnentag, O., Järveoja, J., Peltoniemi, M., Alekseychik, P., Aurela, M., Arslan, A. N., Dinsmore, K., Gianelle, D., Helfter, C., Jackowicz-Korczynski, M., Korrensalo, A., Leith, F., Linkosalmi, M., Lohila, A., Lund, M., Maddison, M., Mammarella, I., Mander, Ü., . . . Peichl, M. (2020). Refining the role of phenology in regulating gross ecosystem productivity across European peatlands. Global Change Biology, 26(2), 876-887. https://doi.org/10.1111/gcb.14905

Kokkonen, N. A. K., Laine, A. M., Laine, J., Vasander, H., Kurki, K., Gong, J., Tuittila, E. S., & Collins, B. (2019). Responses of peatland vegetation to 15-year water level drawdown as mediated by fertility level. Journal of vegetation science, 30(6), 1206-1216. https://doi.org/10.1111/jvs.12794

Korrensalo, A., Alekseychik, P., Hájek, T., Rinne, J., Vesala, T., Mehtätalo, L., Mammarella, I., & Tuittila, E.-S. (2017). Species-specific temporal variation in photosynthesis as a moderator of peatland carbon sequestration. Biogeosciences, 14(2), 257-269. https://doi.org/10.5194/bg-14-257-2017

Kross, A. S. E., Roulet, N. T., Moore, T. R., Lafleur, P. M., Humphreys, E. R., Seaquist, J. W., Flanagan, L. B., & Aurela, M. (2014). Phenology and its role in carbon dioxide exchange processes in northern peatlands. Journal of geophysical research.Biogeosciences, 119(7), 1370-1384. https://doi.org/10.1002/2014JG002666

Laiho, R. (2006). Decomposition in peatlands: Reconciling seemingly contrasting results on the impacts of lowered water levels. Soil Biology and Biochemistry, 38(8), 2011-2024.

Laiho, R., Vasander, H., Timo, P., & Laine, J. (2003). Dynamics of plant-mediated organic matter and nutrient cycling following water-level drawdown in boreal peatlands. Global Biogeochemical Cycles, 17(2), 1053-n/a. https://doi.org/10.1029/2002GB002015

Laine, A., Byrne, K. A., Kiely, G., & Tuittila, E.-S. (2007). Patterns in vegetation and CO2 dynamics along a water level gradient in a lowland blanket bog. Ecosystems, 10(6), 890-905.

Laine, J., Komulainen, V.-M., Laiho, R., Minkkinen, K., Päivänen, J., Rasinmäki, A., Sallantaus, T., Sarkkola, S., Silvan, N., Tolonen, K., Tuittila, E.-S., & Vasander, H. (2004). Lakkasuo : a guide to mire ecosystem. Helsingin yliopisto, metsäekologian laitos.

Leppälä, M., Laine, A. M., Seväkivi, M. L., & Tuittila, E. S. (2011). Differences in CO2 dynamics between successional mire plant communities during wet and dry summers. Journal of vegetation science, 22(2), 357-366.

Lieffers, V., & Rothwell, R. (1987). Effects of drainage on substrate temperature and phenology of some trees and shrubs in an Alberta peatland. Canadian Journal of Forest Research, 17(2), 97-104.

Lohila, A., Minkkinen, K., Aurela, M., Tuovinen, J. P., Penttilä, T., Ojanen, P., & Laurila, T. (2011). Greenhouse gas flux measurements in a forestry-drained peatland indicate a large carbon sink. Biogeosciences, 8(11), 3203-3218. https://doi.org/10.5194/bg-8-3203-2011

Loreau, M. (2010). Linking biodiversity and ecosystems: towards a unifying ecological theory. Philosophical Transactions of the Royal Society B: Biological Sciences, 365(1537), 49-60.

Lund, M., Christensen, T. R., Lindroth, A., & Schubert, P. (2012). Effects of drought conditions on the carbon dioxide dynamics in a temperate peatland. Environmental Research Letters, 7(4), 045704.

Macrae, M. L., Devito, K. J., Strack, M., & Waddington, J. M. (2013). Effect of water table drawdown on peatland nutrient dynamics: implications for climate change. Biogeochemistry, 112(1), 661-677. https://doi.org/10.1007/s10533-012-9730-3

Mäkiranta, P., Laiho, R., Mehtätalo, L., Straková, P., Sormunen, J., Minkkinen, K., Penttilä, T., Fritze, H., & Tuittila, E. S. (2018). Responses of phenology and biomass production of boreal fens to climate warming under different water-table level regimes. Global Change Biology; Glob Chang Biol, 24(3), 944-956. https://doi.org/10.1111/gcb.13934

Monier, E., Sokolov, A., Schlosser, A., Scott, J., & Gao, X. (2013). Probabilistic projections of 21st century climate change over Northern Eurasia. Environmental research letters; Environ.Res.Lett, 8(4), 45008. https://doi.org/10.1088/1748-9326/8/4/045008

Munir, T. M., Xu, B., Perkins, M., & Strack, M. (2014). Responses of carbon dioxide flux and plant biomass to water table drawdown in a treed peatland in northern Alberta: a climate change perspective. Biogeosciences, 11(3), 807-820. https://doi.org/10.5194/bg-11-807-2014

Oksanen, L. (2004). The Devil Lies in Details: Reply to Stuart Hurlbert. Oikos, 104(3), 598-605. https://doi.org/10.1111/j.0030-1299.2004.13266.x

Peichl, M., Gažovič, M., Vermeij, I., De Goede, E., Sonnentag, O., Limpens, J., & Nilsson, M. B. (2018). Peatland vegetation composition and phenology drive the seasonal trajectory of maximum gross primary production. Scientific reports, 8(1), 1-11.

Peichl, M., Öquist, M., Löfvenius, M. O., Ilstedt, U., Sagerfors, J., Grelle, A., Lindroth, A., & Nilsson, M. B. (2014). A 12-year record reveals pre-growing season temperature and

water table level threshold effects on the net carbon dioxide exchange in a boreal fen. Environmental Research Letters, 9(5), 055006.

Peichl, M., Sonnentag, O., & Nilsson, M. B. (2015). Bringing Color into the Picture: Using Digital Repeat Photography to Investigate Phenology Controls of the Carbon Dioxide Exchange in a Boreal Mire. Ecosystems (New York), 18(1), 115-131. https://doi.org/10.1007/s10021-014-9815-z

Rana, P., & Tolvanen, A. (2021). Transferability of 34 red-listed peatland plant species models across boreal vegetation zone. Ecological Indicators, 129. https://doi.org/ARTN 107950

10.1016/j.ecolind.2021.107950

Rinne, J., Tuovinen, J.-P., Klemedtsson, L., Aurela, M., Holst, J., Lohila, A., Weslien, P., Vestin, P., Łakomiec, P., & Peichl, M. (2020). Effect of the 2018 European drought on methane and carbon dioxide exchange of northern mire ecosystems. Philosophical Transactions of the Royal Society B, 375(1810), 20190517.

Riutta, T., Laine, J., & Tuittila, E.-S. (2007). Sensitivity of CO2 exchange of fen ecosystem components to water level variation. Ecosystems, 10(5), 718-733.

Rupp, D., Kane, E. S., Dieleman, C., Keller, J. K., & Turetsky, M. (2019). Plant functional group effects on peat carbon cycling in a boreal rich fen. Biogeochemistry, 144(3), 305-327. https://doi.org/10.1007/s10533-019-00590-5

Silvola, J., Alm, J., Ahlholm, U., Nykanen, H., & Martikainen, P. J. (1996). CO2 fluxes from peat in boreal mires under varying temperature and moisture conditions. The Journal of ecology, 84(2), 219. https://doi.org/10.2307/2261357

Skov, F., & Svenning, C. (2004). Potential impact of climatic change on the distribution of forest herbs in Europe (vol 27, pg 366, 2004). Ecography, 27(6), 827-828. <Go to ISI>://WOS:000225974900014

Steudel, B., Hector, A., Friedl, T., Löfke, C., Lorenz, M., Wesche, M., & Kessler, M. (2012). Biodiversity effects on ecosystem functioning change along environmental stress gradients. Ecology letters, 15(12), 1397-1405.

Straková, P., Penttilä, T., Laine, J., & Laiho, R. (2012). Disentangling direct and indirect effects of water table drawdown on above-and belowground plant litter decomposition: consequences for accumulation of organic matter in boreal peatlands. Global Change Biology, 18(1), 322-335.

Sulman, B. N., Desai, A. R., Saliendra, N. Z., Lafleur, P. M., Flanagan, L. B., Sonnentag, O., Mackay, D. S., Barr, A. G., & Van Der Kamp, G. (2010). CO2fluxes at northern fens

and bogs have opposite responses to inter-annual fluctuations in water table. Geophysical Research Letters, 37(19), n/a-n/a. https://doi.org/10.1029/2010gl044018

Tahvanainen, T. (2011). Abrupt ombrotrophication of a boreal aapa mire triggered by hydrological disturbance in the catchment. The Journal of ecology, 99(2), 404-415. https://doi.org/10.1111/j.1365-2745.2010.01778.x

Tuittila, E. S., Väliranta, M., Laine, J., & Korhola, A. (2007). Quantifying patterns and controls of mire vegetation succession in a southern boreal bog in Finland using partial ordinations. Journal of vegetation science, 18(6), 891-902.

Urbanová, Z., Picek, T., Hájek, T., Bufkova, I., & Tuittila, E.-S. (2012). Vegetation and carbon gas dynamics under a changed hydrological regime in central European peatlands. Plant Ecology & Diversity, 5(1), 89-103.

Väliranta, M., Korhola, A., Seppä, H., Tuittila, E.-S., Sarmaja-Korjonen, K., Laine, J., & Alm, J. (2007). High-resolution reconstruction of wetness dynamics in a southern boreal raised bog, Finland, during the late Holocene: a quantitative approach. The Holocene, 17(8), 1093-1107.

Van Breemen, N. (1995). How Sphagnum bogs down other plants. Trends in ecology & evolution, 10(7), 270-275.

Waddington, J., Morris, P., Kettridge, N., Granath, G., Thompson, D., & Moore, P. (2015). Hydrological feedbacks in northern peatlands. Ecohydrology, 8(1), 113-127.

Wang, H., Tian, J., Chen, H., Ho, M., Vilgalys, R., Bu, Z.-J., Liu, X., & Richardson, C. J. (2021). Vegetation and microbes interact to preserve carbon in many wooded peatlands. Communications Earth & Environment, 2(1), 1-8.

Weltzin, J. F., Bridgham, S. D., Pastor, J., Chen, J., & Harth, C. (2003). Potential effects of warming and drying on peatland plant community composition. Global Change Biology, 9(2), 141-151. https://doi.org/10.1046/j.1365-2486.2003.00571.x

Wilson, D., Alm, J., Riutta, T., Laine, J., Byrne, K. A., Farrell, E. P., & Eeva-Stiina, T. (2007). A High Resolution Green Area Index for Modelling the Seasonal Dynamics of Co_2 Exchange in Peatland Vascular Plant Communities. Plant Ecology, 190(1), 37-51. https://doi.org/10.1007/s11258-006-9189-1

Wu, J., & Roulet, N. T. (2014). Climate change reduces the capacity of northern peatlands to absorb the atmospheric carbon dioxide: The different responses of bogs and fens. Global Biogeochemical Cycles, 28(10), 1005-1024. https://doi.org/10.1002/2014GB004845

Yu, Z., Beilman, D. W., Frolking, S., MacDonald, G. M., Roulet, N. T., Camill, P., & Charman, D. J. (2011). Peatlands and Their Role in the Global Carbon Cycle. Eos (Washington, D.C.), 92(12), 97-98. https://doi.org/10.1029/2011EO120001

Yu, Z., Loisel, J., Brosseau, D. P., Beilman, D. W., & Hunt, S. J. (2010). Global peatland dynamics since the Last Glacial Maximum. Geophysical Research Letters, 37(13), n/a. https://doi.org/10.1029/2010GL043584

Zhang, H., Väliranta, M., Piilo, S., Amesbury, M. J., Aquino-López, M. A., Roland, T. P., Salminen-Paatero, S., Paatero, J., Lohila, A., & Tuittila, E. S. (2020). Decreased carbon accumulation feedback driven by climate-induced drying of two southern boreal bogs over recent centuries. Global Change Biology, 26(4), 2435-2448.

7 APPENDICES

Appendix 1. Pairwise comparisons between all log transformed model estimates for each parameter.

a. LAIMAX

Contrast	Estimate	SE	*t* ratio	*p* value
2017 control meso - 2021 control meso	-0.1902	0.1211	-1.5701	0.9190
2017 control meso - 2017 wld meso	1.5745	0.2117	7.4370	<0.0001
2017 control meso - 2021 wld meso	0.6841	0.1979	3.4564	0.0293
2017 control meso - 2017 control oligo	0.5159	0.1401	3.6812	0.0137
2017 control meso - 2021 control oligo	0.3257	0.1832	1.7781	0.8292
2017 control meso - 2017 wld oligo	0.8340	0.1724	4.8377	0.0001
2017 control meso - 2021 wld oligo	-0.0565	0.1654	-0.3415	1.0000
2017 control meso - 2017 control ombro	1.3414	0.1556	8.6178	<0.0001
2017 control meso - 2021 control ombro	1.1512	0.1933	5.9554	<0.0001
2017 control meso - 2017 wld ombro	1.7124	0.1964	8.7180	<0.0001
2017 control meso - 2021 wld ombro	0.8220	0.1827	4.4988	0.0005
2021 control meso - 2017 wld meso	1.7647	0.2119	8.3287	<0.0001
2021 control meso - 2021 wld meso	0.8743	0.1980	4.4157	0.0008
2021 control meso - 2017 control oligo	0.7061	0.1873	3.7699	0.0100
2021 control meso - 2021 control oligo	0.5159	0.1401	3.6812	0.0137
2021 control meso - 2017 wld oligo	1.0242	0.1727	5.9293	<0.0001
2021 control meso - 2021 wld oligo	0.1337	0.1656	0.8076	0.9997
2021 control meso - 2017 control ombro	1.5316	0.2011	7.6160	<0.0001
2021 control meso - 2021 control ombro	1.3414	0.1556	8.6178	<0.0001
2021 control meso - 2017 wld ombro	1.9026	0.1967	9.6706	<0.0001
2021 control meso - 2021 wld ombro	1.0122	0.1829	5.5330	<0.0001
2017 wld meso - 2021 wld meso	-0.8904	0.1433	-6.2159	<0.0001

2017 wld meso - 2017 control oligo	-1.0586	0.2129	-4.9714	0.0001
2017 wld meso - 2021 control oligo	-1.2488	0.2113	-5.9100	<0.0001
2017 wld meso - 2017 wld oligo	-0.7406	0.1815	-4.0809	0.0031
2017 wld meso - 2021 wld oligo	-1.6310	0.2382	-6.8475	<0.0001
2017 wld meso - 2017 control ombro	-0.2332	0.2245	-1.0386	0.9967
2017 wld meso - 2021 control ombro	-0.4234	0.2212	-1.9138	0.7501
2017 wld meso - 2017 wld ombro	0.1379	0.2001	0.6889	0.9999
2017 wld meso - 2021 wld ombro	-0.7526	0.2470	-3.0463	0.0990
2021 wld meso - 2017 control oligo	-0.1682	0.1994	-0.8434	0.9995
2021 wld meso - 2021 control oligo	-0.3584	0.1976	-1.8142	0.8096
2021 wld meso - 2017 wld oligo	0.1499	0.2240	0.6691	0.9999
2021 wld meso - 2021 wld oligo	-0.7406	0.1815	-4.0809	0.0031
2021 wld meso - 2017 control ombro	0.6573	0.2119	3.1015	0.0851
2021 wld meso - 2021 control ombro	0.4671	0.2083	2.2419	0.5200
2021 wld meso - 2017 wld ombro	1.0283	0.2452	4.1936	0.0019
2021 wld meso - 2021 wld ombro	0.1379	0.2001	0.6889	0.9999
2017 control oligo - 2021 control oligo	-0.1902	0.1211	-1.5701	0.9190
2017 control oligo - 2017 wld oligo	0.3181	0.1730	1.8384	0.7959
2017 control oligo - 2021 wld oligo	-0.5724	0.1662	-3.4434	0.0305
2017 control oligo - 2017 control ombro	0.8255	0.1551	5.3210	<0.0001
2017 control oligo - 2021 control ombro	0.6353	0.1949	3.2602	0.0539
2017 control oligo - 2017 wld ombro	1.1965	0.1970	6.0742	<0.0001
2017 control oligo - 2021 wld ombro	0.3061	0.1835	1.6679	0.8818
2021 control oligo - 2017 wld oligo	0.5083	0.1711	2.9701	0.1210
2021 control oligo - 2021 wld oligo	-0.3822	0.1641	-2.3284	0.4579
2021 control oligo - 2017 control ombro	1.0157	0.1988	5.1094	<0.0001
2021 control oligo - 2021 control ombro	0.8255	0.1551	5.3210	<0.0001
2021 control oligo - 2017 wld ombro	1.3867	0.1953	7.0986	<0.0001
2021 control oligo - 2021 wld ombro	0.4963	0.1816	2.7323	0.2140
2017 wld oligo - 2021 wld oligo	-0.8904	0.1433	-6.2159	<0.0001
2017 wld oligo - 2017 control ombro	0.5074	0.1868	2.7163	0.2216
2017 wld oligo - 2021 control ombro	0.3172	0.1830	1.7338	0.8517
2017 wld oligo - 2017 wld ombro	0.8784	0.1640	5.3549	<0.0001
2017 wld oligo - 2021 wld ombro	-0.0120	0.2112	-0.0568	1.0000
2021 wld oligo - 2017 control ombro	1.3978	0.1808	7.7322	<0.0001
2021 wld oligo - 2021 control ombro	1.2076	0.1767	6.8348	<0.0001
2021 wld oligo - 2017 wld ombro	1.7689	0.2242	7.8900	<0.0001
2021 wld oligo - 2021 wld ombro	0.8784	0.1640	5.3549	<0.0001
2017 control ombro - 2021 control ombro	-0.1902	0.1211	-1.5701	0.9190
2017 control ombro - 2017 wld ombro	0.3710	0.2088	1.7767	0.8300
2017 control ombro - 2021 wld ombro	-0.5194	0.1964	-2.6447	0.2582
2021 control ombro - 2017 wld ombro	0.5612	0.2054	2.7321	0.2141
2021 control ombro - 2021 wld ombro	-0.3292	0.1927	-1.7087	0.8636
2017 wld ombro - 2021 wld ombro	-0.8904	0.1433	-6.2159	<0.0001

b. DMAX

Contrast	Estimate	SE	*t* ratio	*p* value
2017 meso control - 2021 meso control	0.2238	0.0382	5.8542	<0.0001
2017 meso control - 2017 oligo control	0.0828	0.0380	2.1798	0.5652
2017 meso control - 2021 oligo control	0.0683	0.0464	1.4703	0.9478
2017 meso control - 2017 ombro control	-0.0452	0.0812	-0.5567	1.0000
2017 meso control - 2021 ombro control	0.0426	0.0573	0.7443	0.9999
2017 meso control - 2017 meso wld	0.1063	0.0362	2.9351	0.1323
2017 meso control - 2021 meso wld	0.3300	0.0460	7.1735	<0.0001
2017 meso control - 2017 oligo wld	0.1891	0.0518	3.6524	0.0151
2017 meso control - 2021 oligo wld	0.1746	0.0368	4.7441	0.0002
2017 meso control - 2017 ombro wld	0.0611	0.0812	0.7527	0.9998
2017 meso control - 2021 ombro wld	0.1489	0.0548	2.7162	0.2217
2021 meso control - 2017 oligo control	-0.1409	0.0424	-3.3263	0.0441
2021 meso control - 2021 oligo control	-0.1555	0.0446	-3.4835	0.0268
2021 meso control - 2017 ombro control	-0.2690	0.0815	-3.3001	0.0478
2021 meso control - 2021 ombro control	-0.1811	0.0570	-3.1770	0.0688
2021 meso control - 2017 meso wld	-0.1175	0.0585	-2.0062	0.6891
2021 meso control - 2021 meso wld	0.1063	0.0362	2.9351	0.1323
2021 meso control - 2017 oligo wld	-0.0346	0.0607	-0.5704	1.0000
2021 meso control - 2021 oligo wld	-0.0492	0.0430	-1.1449	0.9924
2021 meso control - 2017 ombro wld	-0.1627	0.0854	-1.9052	0.7556
2021 meso control - 2021 ombro wld	-0.0748	0.0602	-1.2419	0.9853
2017 oligo control - 2021 oligo control	-0.0145	0.0495	-0.2937	1.0000
2017 oligo control - 2017 ombro control	-0.1280	0.0831	-1.5399	0.9286
2017 oligo control - 2021 ombro control	-0.0402	0.0600	-0.6698	0.9999
2017 oligo control - 2017 meso wld	0.0235	0.0532	0.4414	1.0000
2017 oligo control - 2021 meso wld	0.2472	0.0503	4.9196	0.0001
2017 oligo control - 2017 oligo wld	0.1063	0.0362	2.9351	0.1323
2017 oligo control - 2021 oligo wld	0.0917	0.0415	2.2089	0.5441
2017 oligo control - 2017 ombro wld	-0.0217	0.0835	-0.2601	1.0000
2017 oligo control - 2021 ombro wld	0.0661	0.0583	1.1349	0.9930
2021 oligo control - 2017 ombro control	-0.1135	0.0813	-1.3963	0.9639
2021 oligo control - 2021 ombro control	-0.0256	0.0554	-0.4623	1.0000
2021 oligo control - 2017 meso wld	0.0380	0.0747	0.5090	1.0000
2021 oligo control - 2021 meso wld	0.2618	0.0690	3.7936	0.0091
2021 oligo control - 2017 oligo wld	0.1208	0.0762	1.5862	0.9135
2021 oligo control - 2021 oligo wld	0.1063	0.0362	2.9351	0.1323
2021 oligo control - 2017 ombro wld	-0.0072	0.0933	-0.0770	1.0000
2021 oligo control - 2021 ombro wld	0.0807	0.0701	1.1513	0.9921
2017 ombro control - 2021 ombro control	0.0879	0.0893	0.9840	0.9980
2017 ombro control - 2017 meso wld	0.1515	0.0961	1.5773	0.9166
2017 ombro control - 2021 meso wld	0.3753	0.0928	4.0422	0.0036
2017 ombro control - 2017 oligo wld	0.2343	0.0973	2.4080	0.4028
2017 ombro control - 2021 oligo wld	0.2198	0.0844	2.6040	0.2805

2017 ombro control - 2017 ombro wld	0.1063	0.0362	2.9351	0.1323
2017 ombro control - 2021 ombro wld	0.1941	0.0949	2.0448	0.6623
2021 ombro control - 2017 meso wld	0.0637	0.0786	0.8095	0.9997
2021 ombro control - 2021 meso wld	0.2874	0.0741	3.8776	0.0067
2021 ombro control - 2017 oligo wld	0.1465	0.0801	1.8277	0.8020
2021 ombro control - 2021 oligo wld	0.1319	0.0621	2.1237	0.6060
2021 ombro control - 2017 ombro wld	0.0184	0.0977	0.1887	1.0000
2021 ombro control - 2021 ombro wld	0.1063	0.0362	2.9351	0.1323
2017 meso wld - 2021 meso wld	0.2238	0.0382	5.8542	<0.0001
2017 meso wld - 2017 oligo wld	0.0828	0.0380	2.1798	0.5652
2017 meso wld - 2021 oligo wld	0.0683	0.0464	1.4703	0.9478
2017 meso wld - 2017 ombro wld	-0.0452	0.0812	-0.5567	1.0000
2017 meso wld - 2021 ombro wld	0.0426	0.0573	0.7443	0.9999
2021 meso wld - 2017 oligo wld	-0.1409	0.0424	-3.3263	0.0441
2021 meso wld - 2021 oligo wld	-0.1555	0.0446	-3.4835	0.0268
2021 meso wld - 2017 ombro wld	-0.2690	0.0815	-3.3001	0.0478
2021 meso wld - 2021 ombro wld	-0.1811	0.0570	-3.1770	0.0688
2017 oligo wld - 2021 oligo wld	-0.0145	0.0495	-0.2937	1.0000
2017 oligo wld - 2017 ombro wld	-0.1280	0.0831	-1.5399	0.9286
2017 oligo wld - 2021 ombro wld	-0.0402	0.0600	-0.6698	0.9999
2021 oligo wld - 2017 ombro wld	-0.1135	0.0813	-1.3963	0.9639
2021 oligo wld - 2021 ombro wld	-0.0256	0.0554	-0.4623	1.0000
2017 ombro wld - 2021 ombro wld	0.0879	0.0893	0.9840	0.9980

c. scale

Contrast	Estimate	SE	*t* ratio	*p* value
2017 control meso - 2021 control meso	-0.2772	0.0829	-3.3441	0.0418
2017 control meso - 2017 wld meso	0.5242	0.3197	1.6397	0.8934
2017 control meso - 2021 wld meso	0.4836	0.1275	3.7929	0.0092
2017 control meso - 2017 control oligo	0.1817	0.0936	1.9417	0.7322
2017 control meso - 2021 control oligo	-0.4780	0.1049	-4.5560	0.0004
2017 control meso - 2017 wld oligo	-0.4584	0.1438	-3.1887	0.0665
2017 control meso - 2021 wld oligo	-0.1639	0.0793	-2.0675	0.6463
2017 control meso - 2017 control ombro	-0.2081	0.1992	-1.0450	0.9965
2017 control meso - 2021 control ombro	-0.1001	0.1775	-0.5637	1.0000
2017 control meso - 2017 wld ombro	-0.0525	0.2116	-0.2480	1.0000
2017 control meso - 2021 wld ombro	0.0832	0.1342	0.6198	1.0000
2021 control meso - 2017 wld meso	0.8014	0.3198	2.5060	0.3388
2021 control meso - 2021 wld meso	0.7608	0.1299	5.8580	<0.0001
2021 control meso - 2017 control oligo	0.4589	0.0974	4.7136	0.0002
2021 control meso - 2021 control oligo	-0.2007	0.1064	-1.8862	0.7674
2021 control meso - 2017 wld oligo	-0.1812	0.1463	-1.2384	0.9856
2021 control meso - 2021 wld oligo	0.1133	0.0833	1.3609	0.9701
2021 control meso - 2017 control ombro	0.0691	0.2013	0.3432	1.0000

2021 control meso - 2021 control ombro	0.1771	0.1782	0.9939	0.9978
2021 control meso - 2017 wld ombro	0.2247	0.2133	1.0536	0.9963
2021 control meso - 2021 wld ombro	0.3604	0.1365	2.6407	0.2603
2017 wld meso - 2021 wld meso	-0.0407	0.3275	-0.1242	1.0000
2017 wld meso - 2017 control oligo	-0.3425	0.3237	-1.0583	0.9961
2017 wld meso - 2021 control oligo	-1.0022	0.3256	-3.0784	0.0907
2017 wld meso - 2017 wld oligo	-0.9826	0.3389	-2.8993	0.1446
2017 wld meso - 2021 wld oligo	-0.6881	0.3204	-2.1476	0.5887
2017 wld meso - 2017 control ombro	-0.7323	0.3674	-1.9934	0.6978
2017 wld meso - 2021 control ombro	-0.6243	0.3562	-1.7527	0.8423
2017 wld meso - 2017 wld ombro	-0.5767	0.3697	-1.5598	0.9224
2017 wld meso - 2021 wld ombro	-0.4410	0.3393	-1.2996	0.9789
2021 wld meso - 2017 control oligo	-0.3019	0.1369	-2.2044	0.5473
2021 wld meso - 2021 control oligo	-0.9615	0.1445	-6.6532	<0.0001
2021 wld meso - 2017 wld oligo	-0.9420	0.1762	-5.3471	<0.0001
2021 wld meso - 2021 wld oligo	-0.6475	0.1272	-5.0904	<0.0001
2021 wld meso - 2017 control ombro	-0.6917	0.2232	-3.0992	0.0857
2021 wld meso - 2021 control ombro	-0.5836	0.2033	-2.8706	0.1552
2021 wld meso - 2017 wld ombro	-0.5360	0.2356	-2.2748	0.4962
2021 wld meso - 2021 wld ombro	-0.4004	0.1666	-2.4037	0.4057
2017 control oligo - 2021 control oligo	-0.6596	0.1162	-5.6749	<0.0001
2017 control oligo - 2017 wld oligo	-0.6401	0.1531	-4.1795	0.0021
2017 control oligo - 2021 wld oligo	-0.3456	0.0937	-3.6888	0.0133
2017 control oligo - 2017 control ombro	-0.3898	0.2052	-1.8999	0.7589
2017 control oligo - 2021 control ombro	-0.2818	0.1849	-1.5241	0.9334
2017 control oligo - 2017 wld ombro	-0.2341	0.2174	-1.0771	0.9955
2017 control oligo - 2021 wld ombro	-0.0985	0.1433	-0.6874	0.9999
2021 control oligo - 2017 wld oligo	0.0196	0.1610	0.1215	1.0000
2021 control oligo - 2021 wld oligo	0.3140	0.1017	3.0878	0.0884
2021 control oligo - 2017 control ombro	0.2698	0.2092	1.2898	0.9801
2021 control oligo - 2021 control ombro	0.3779	0.1876	2.0143	0.6836
2021 control oligo - 2017 wld ombro	0.4255	0.2232	1.9065	0.7548
2021 control oligo - 2021 wld ombro	0.5612	0.1505	3.7277	0.0116
2017 wld oligo - 2021 wld oligo	0.2945	0.1431	2.0577	0.6532
2017 wld oligo - 2017 control ombro	0.2503	0.2335	1.0718	0.9957
2017 wld oligo - 2021 control ombro	0.3583	0.2146	1.6698	0.8810
2017 wld oligo - 2017 wld ombro	0.4059	0.2404	1.6889	0.8726
2017 wld oligo - 2021 wld ombro	0.5416	0.1811	2.9900	0.1149
2021 wld oligo - 2017 control ombro	-0.0442	0.1999	-0.2212	1.0000
2021 wld oligo - 2021 control ombro	0.0638	0.1774	0.3599	1.0000
2021 wld oligo - 2017 wld ombro	0.1114	0.2121	0.5255	1.0000
2021 wld oligo - 2021 wld ombro	0.2471	0.1340	1.8446	0.7923
2017 control ombro - 2021 control ombro	0.1080	0.2476	0.4363	1.0000
2017 control ombro - 2017 wld ombro	0.1557	0.2721	0.5720	1.0000
2017 control ombro - 2021 wld ombro	0.2913	0.2269	1.2838	0.9808
2021 control ombro - 2017 wld ombro	0.0476	0.2642	0.1802	1.0000

2021 control ombro - 2021 wld ombro	0.1833	0.2084	0.8793	0.9993
2017 wld ombro - 2021 wld ombro	0.1357	0.2333	0.5815	1.0000

Appendix 2. Log transformed parameter estimates for leaf area maximum (LAIMAX), timing of LAIMAX (DMAX) and Shape, based on a model including all the interaction levels between predictors. For all parameters the intercept is the mesotrophic control site in 2017 (mesocontrol2017) to which all other sites, WLD treatment and year 2021 are compared. DMAX values are days since Julian date 110, set as the start of the growing season. The random effects included in the model are displayed at bottom.

Fixed predictors	Value	Std. error	t-value	*p*-value
LAIMAX (m^2 m^{-2})				
Intercept (mesocontrol2017)	0.026776	0.1404973	0.19058	0.8489
2021	-0.007946	0.1994916	-0.03983	0.9682
wld	-1.435513	0.2987365	-4.80528	0
oligo	-0.621434	0.2008984	-3.09328	0.0021
ombro	-1.578809	0.2323094	-6.79615	0
2021*wld	0.563239	0.3771809	1.49329	0.1361
2021*oligo	0.207124	0.2812146	0.73654	0.4618
2021*ombro	0.505647	0.3157547	1.60139	0.11
wld*oligo	1.01648	0.3650171	2.78474	0.0056
wld*ombro	1.506281	0.4036345	3.73179	0.0002
2021*wld*oligo	0.33453	0.4717916	0.70906	0.4787
2021*wld*ombro	-0.577573	0.5198512	-1.11103	0.2672
DMAX (Julian date)				
Intercept (mesocontrol2017)	4.518172	0.024034	187.99079	0
2021	-0.240066	0.0422775	-5.67834	0
wld	0.074124	0.0596041	1.2436	0.2143
oligo	-0.055439	0.0395217	-1.40274	0.1614
ombro	-0.001019	0.1201207	-0.00848	0.9932
2021*wld	-0.056802	0.0964105	-0.58917	0.556
2021*oligo	0.3868	0.1350505	2.86411	0.0044
2021*ombro	0.405175	0.1511679	2.6803	0.0076
wld*oligo	-0.293801	0.1169946	-2.51123	0.0124
wld*ombro	-0.075741	0.1526235	-0.49626	0.62
2021*wld*oligo	0.009778	0.188934	0.05176	0.9587
2021*wld*ombro	-0.348456	0.1977945	-1.76171	0.0788
Shape				
Intercept (mesocontrol2017)	-0.68046	0.0551348	-12.34175	0

2021	0.294943	0.0831289	3.54802	0.0004
wld	-0.852373	0.3001751	-2.83958	0.0047
oligo	-0.184352	0.0948087	-1.94447	0.0525
ombro	0.236727	0.2230361	1.06138	0.2891
2021*wld	0.134169	0.335836	0.39951	0.6897
2021*oligo	0.49048	0.1704186	2.87809	0.0042
2021*ombro	-0.539889	0.3183769	-1.69575	0.0906
wld*oligo	1.527297	0.3374564	4.52591	0
wld*ombro	0.515827	0.4103011	1.25719	0.2093
2021*wld*oligo	-1.257911	0.3946454	-3.18745	0.0015
2021*wld*ombro	0.078006	0.5010489	0.15569	0.8764
Random part	StDev			
LAIMAX (m^2 m^{-2})				
$\sigma(b_p)$	0.3738721			
$\sigma(e_{pm})$	0.1331622			

Appendix 3. Full scientific names of species abbreviations used in Figure 15

Abbreviation	Specific name	Abbreviation	Specific name	Abbreviation	Specific name
Agrost	*Agrostis spp.*	Melamp	*Melampyrum spp.*	Sphsqu	*Sphagnum squarrosum*
Andpol	*Andromeda polifolia*	Mentri	*Menyanthes trifoliata*	Sphsub	*Sphagnum subsecundum*
Aulpal	*Aulacomium palustre*	Mylano	*Mylia anomala*	Sphter	*Sphagnum teres*
Betnan	*Betula nana*	Picabi	*Picea abies*	Sphwar	*Sphagnum warnstorfi*
Betpub	*Betula pubescens*	Pinsyl	*Pinus sylvestris*	Sphwul	*Sphagnum wulfianum*
Calama	*Calamagrostis*	Plesch	*Pleurozium schreberi*	Trialp	*Trichophorum alpinum*
Carcho	*Carex chordorrhiza*	Poljun	*Polytrichum juniperinum*	Trices	*Trichophorum cespitosum*
Carech	*Carex echinata*	Polstr	*Polytrichum strictum*	Trieur	*Trientalis europea*
Carlas	*Carex lasiocarpa*	Potpal	*Potentilla palustris*	Utrint	*Utricularia intermedia*
Carlim	*Carex limosa*	Rhysub	*Rhytidiadelphus subpinnatus*	Vacoxy	*Vaccinium ocycoccus*
Carliv	*Carex livida*	Rubcha	*Rubus chamaemorus*	Vaculi	*Vaccinium uliginosum*
Carmag	*Carex magellanicum*	Schpal	*Scheuzeria palustris*	Viopal	*Viola palustris*
Carpau	*Carex pauciflora*	Sphang	*Sphagnum angustifolium*	Warnst	*Warnstorfia spparex*
Carros	*Carex rostrata*	Sphbal	*Sphagnum balticum*		
Cirpal	*Cirsium palustre*	Sphcap	*Sphagnum capillifolium*		
Dacinc	*Dactylorhiza incarnata*	Sphcus	*Sphagnum cuspidatum*		
Dacmac	*Dactylorhiza maculata*	Sphdiv	*Sphagnum divinum*		
Dicpol	*Dicranum polysetum*	Sphfal	*Sphagnum fallax*		
Drolon	*Drosera longifolia*	Sphfus	*Sphagnum fuscum*		
Drorot	*Drosera rotundifolia*	Sphmaj	*Sphagnum majus*		
Empnig	*Empetrum nigrum*	Sphmed	*Sphagnum medium*		
Eriang	*Eriophorum angustifolium*	Sphpap	*Sphagnum papillosum*		
Erivag	*Eriophorum vaginatum*	Sphrub	*Sphagnum rubellum*		
Marcha	*Marchantiophyta spp.*	Sphrus	*Sphagnum russowi*		